DOI: 10.11817/j.ysxb.1004.0609.2021-42136

功率互连全IMC焊点的研究进展

刘 聪[1]，甘贵生[1,2]，江兆琪[1]，黄 天[1]，马 鹏[1]，陈仕琦[1]，
许乾柱[1]，包成利[1]，程大勇[2]，吴懿平[3]

(1. 重庆理工大学 重庆特种焊接材料与技术高校工程技术研究中心，重庆 400054；
2. 金龙精密铜管集团股份有限公司，重庆 404000；
3. 华中科技大学 材料科学与工程学院，武汉 430074)

摘 要：全金属间化合物焊点具有“低温制备，高温服役”技术优势，成为最可能替代用于高温环境的高铅焊料、Au基焊料等连接材料。本文概述了低温烧结、固液互扩散键合技术、瞬态液相连接等方法制备全金属间化合物(IMC)焊点的特点，综述了Cu/Sn、Cu/In、Sn/Ag、Sn/Ni等体系制备全IMC焊点的研究进展，指出键合时间太长、相变会产生孔洞等缺陷是制约IMC生产应用的主要问题，认为应结合Cu-Cu接头的结构特点和材料性能，在焊料体系方面开发更多基于Sn基、Cu基、Sn-Cu基二元或三元焊料体系，更多地关注焊料的状态、尺寸、制备方法；在制备方法方面，把母材和焊料构造为一个冷热微循环，对焊料进行如飞秒激光、局部激光、感应加热等瞬态、局部高功率加热，同时对母材进行高功率制冷，适当辅助振动和压力能增加碰撞扩散几率和缩短扩散距离，就能快速获得单一高可靠性全IMC焊点。

关键词：全金属间化合物；高温焊料；制备方法；焊料体系；冷热微循环
文章编号：1004-0609(2022)-10-2876-21 **中图分类号**：TG425.1 **文献标志码**：A

引文格式：刘 聪, 甘贵生, 江兆琪, 等. 功率互连全IMC焊点的研究进展[J]. 中国有色金属学报, 2022, 32(10): 2876−2896. DOI: 10.11817/j.ysxb.1004.0609.2021-42136

LIU Cong, GAN Gui-sheng, JIANG Zhao-qi, et al. Progress advances in full IMC solder joints for power electronic[J]. The Chinese Journal of Nonferrous Metals, 2022, 32(10): 2876 − 2896. DOI: 10.11817/j.ysxb.1004.0609.2021-42136

第三代宽禁带半导体碳化硅(SiC)和氮化镓(GaN)等因其优异性能而备受青睐，随着半导体器件功率密度的增加，越来越多的器件被要求应用于高温环境(＞300 ℃)[1−3]。基于《欧盟关于废弃电子电气设备的指令》(WEEE)和《关于限制在电子电器设备中使用某些有害成分的指令》(RoHS)无铅禁令，锡铅共晶焊料的使用受到严格限制，高铅焊料(Pb-5Sn/Pb-10Sn)也仅能应用于军事、航空及空间等高温豁免领域[4]。自无铅化以来，业界就踏上了追寻高温焊料无铅化之旅，但到目前为止尚未发现工作温度超过300 ℃的优异服役性能的无铅焊料。基于此，国内外学者主要是通过以下方法进行研究：第一是研发高温无铅焊料，主要集中在Au、Zn和Bi基焊料[5−10]，但由于Au基焊料成本太高，Zn基焊料熔化温度高、耐腐蚀差，Bi基焊料导热系数低、易粗化、脆性大等缺点[11]，限制了它们在

基金项目：国家自然科学基金资助项目(61974013，61774066)；重庆市自然科学基金资助项目(cstc2020jcyj-msxmX0819)；重庆市教委科技项目重点项目(KJZD-K202101101)；重庆市高校创新研究群体资助项目(CXQT20023)；重庆理工大学研究生创新项目(clgycx20201001，clgycx20201002)
收稿日期：2021-08-03；**修订日期**：2021-11-09
通信作者：甘贵生，博士，教授；电话：023-62563178；E-mail：ggs@cqut.edu.cn

高温领域中的应用；第二是基于全金属间化合物(IMC)熔点一般都高于焊料，采用低温烧结法[12]、固液互扩散键合技术(SLID)[13]、瞬态液相连接法(TLP)[14−15]等方法低温制备高熔点的全IMC接头。如采用低温烧结法以Cu@Sn (Cu颗粒表面镀Sn)+Cu颗粒为中间层，在(200 ℃+10 MPa+20 min)条件下制备了网状Cu_3Sn+Cu颗粒接头[16]。MEYER等[13]在惰性氛围中以SnAg作为中间层，通过固液互扩散键合技术(SLID)在(260 ℃+1200 s)条件下成功制备了Cu_6Sn_5+Ag_3Sn+Cu_3Sn IMC接头。BORDÈRE等[17]采用瞬态液相连接法(TLP)在(250 ℃+5 kPa+120 min)条件下成功制备了Cu_3Sn+Cu_6Sn_5全IMC接头。

目前，制备全IMC接头的焊料体系主要有Cu-Sn、Cu-In、Sn-Ag、Sn-Ni和Sn-Bi焊料等[18−27]。Cu-Sn体系焊料具有成本低、导电性好等优点，但其熔化温度高，导致其热可靠性能差，同时，Cu过量会导致焊料出现粗化结晶物[28−29]。Cu-In体系焊料熔化温度低(In熔点156.6 ℃)，延展性好，扩散速率快，但存在着蠕变性能差、易氧化、成本较高等缺点，故只能应用在一些特定的低温互连领域[30−31]。Sn-Ag体系焊料导电性能和抗蠕变性能优异，但由于其熔点较高(221 ℃)，在Cu基体上润湿性差，且块状Ag_3Sn相会影响焊点的性能，导致其在高温领域中应用受到了一定的限制[32−33]。Ni元素可以细化晶粒，提高焊料的塑性，但Ni扩散速度较慢，故Sn-Ni体系焊料一般作为基板的扩散阻挡层[34−35]。Sn-Bi体系焊料由于其熔点与Sn-Pb共晶焊料相近，蠕变特性好，是低温互连的理想材料，但其较差的延展性和大的脆性限制了其广泛应用[36−37]。基于全IMC焊点具有“低温制备，高温服役”的巨大优势，本文作者对全IMC焊点的制备方法、材料体系和综合性能进行总结，特别是指出现有技术制备全IMC焊点的不足，提出新的解决思路和发展方向。

1　全IMC焊点制备方法研究进展

1.1　低温烧结法制备全IMC焊点

低温烧结过程不发生相变，颗粒之间只是通过固态扩散的方式实现彼此间的有效连接。因此，烧结后其微观组织会更加致密，从而具有优良的导热、导电和力学性能。低温烧结法一般都是采用Cu-Ag、Sn-Ni、Cu-Sn体系焊料，研究较多的是Cu-Sn体系。如ZHONG等[12]在200 ℃和5 MPa的真空条件下烧结纳米Cu_6Sn_5膏体20 min，制备完全由Cu_6Sn_5的组成全IMC接头，接头无任何明显的空隙。通过在250 ℃放电等离子烧结铜箔(0.1 mm厚)和锡箔(0.015 mm厚)获得Cu/Cu_3Sn/Cu_6Sn_5/Cu_3Sn/Cu接头，350 ℃时则获得Cu/Cu_3Sn/Cu焊点[38]。将$Cu_{10}Sn_3$纳米颗粒在200 ℃和10 MPa的真空条件下热压烧结20 min，制备了全$Cu_{10}Sn_3$接头，但其接头中出现大量裂纹；升高到300 ℃时，可获得均匀的全$Cu_{10}Sn_3$接头[39]。采用热压烧结$Cu_{10}Sn_3$纳米颗粒制备了Cu/$Cu_{10}Sn_3$/Cu接头，260 ℃烧结时$Cu_{10}Sn_3$与Cu基体的界面处存在较大的孔洞和裂纹，升高烧结温度时孔洞面积逐渐变小，300 ℃烧结时大的孔洞和裂纹消失，接头为致密饱满的$Cu_{10}Sn_3$接头[40]。由于烧结温度远低于烧结后材料的熔点，即在低温条件下制备IMC焊点能在高温条件下使用，但烧结很容易产生孔洞和裂纹。

1.2　固液互扩散键合制备全IMC焊点

固液互扩散键合(SLID)是采用低温钎料锡或铟，在较低温度下就可键合，小尺寸焊点全部由金属间化合物组成。固液互扩散键合的研究主要集中在Cu-Sn、Ni-Sn、Ag-In和Ag-Sn等体系。键合温度和压力是影响焊点接头性能及组织的重要因素，如采用锡箔(30 μm)作为中间层，在300 ℃和0.05 N压力下，保温16 h可获得单一Cu_3Sn全IMC接头；温度下降到240 ℃和270 ℃时，其焊点由Cu_6Sn_5和Cu_3Sn两相组成[41]。将Cu/Sn(6 μm)/Cu互连结构在260 ℃和1 N压力下，保温180 min后其接头由Cu_3Sn+Cu_6Sn_5组成；当保温时间增加至300 min时可获得完整的Cu_3Sn接头(见图1)[42]。在260 ℃和0.04 MPa压力下，Cu/Sn(6 μm)/Cu互连结构保温120 min时，其接头完全由Cu_3Sn+Cu_6Sn_5组成；当保温时间增加至300 min时，获得了单一Cu_3Sn接头(见图2)[43]。采用Sn-0.7Cu锡膏作为中间层，在300 ℃和0.2 MPa压力下，键合1 h后获得由Cu_6Sn_5+Cu_3Sn组成的接头；在2 MPa压力下，键合2 h时接头由无孔洞全Cu_3Sn组成(见图3)[44]。在240 ℃和0.05 N压力下，Cu/Sn(30 μm)/Cu互连结构保温720 min可获得含有孔洞的Cu_6Sn_5+Cu_3Sn接

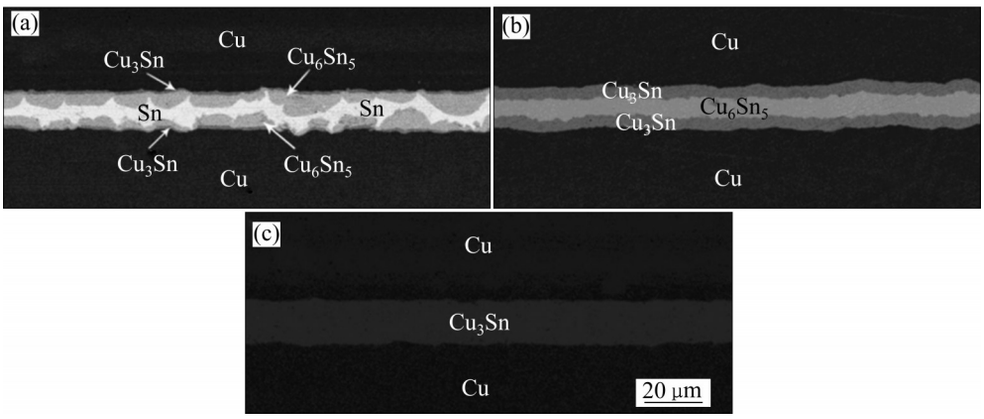

图1 保温不同时间下Cu/Sn/Cu互连结构键合后的SEM像[42]

Fig. 1 SEM images of Cu/Sn/Cu interconnect structure bonding for different time[42]: (a) 50 min; (b) 180 min; (c) 300 min

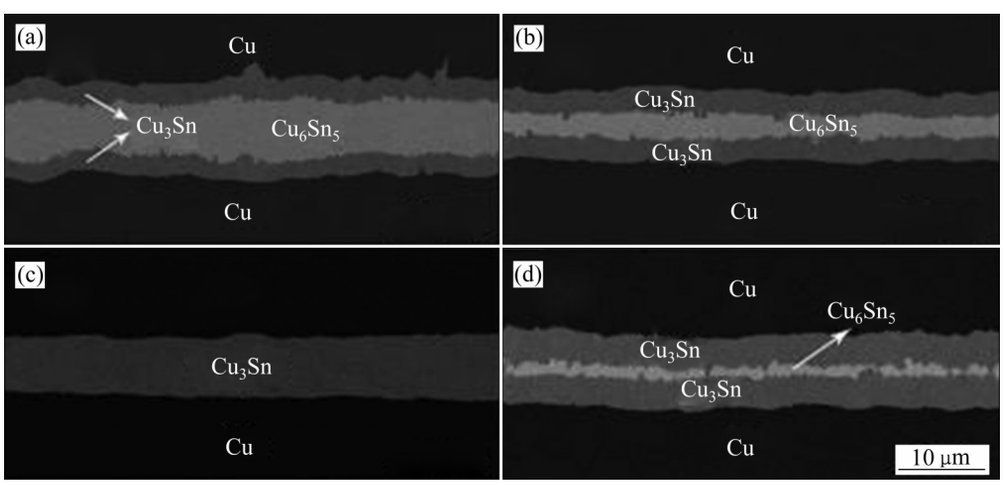

图2 260 ℃，0.04 MPa条件下保温不同时间下Cu/Sn/Cu接头焊后的SEM像[43]

Fig. 2 SEM images of Cu/Sn/Cu joints after welding held at 260 ℃ and 0.04 MPa for different time[43]: (a) 120 min; (b) 180 min; (c) 240 min; (d) 300 min

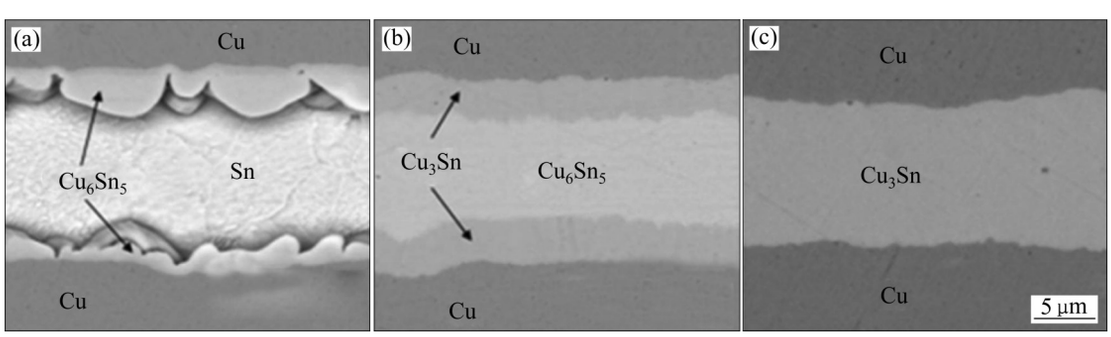

图3 不同键合条件Cu/Sn/Cu SLID接头的SEM像[44]

Fig. 3 SEM images of Cu/Sn/Cu SLID joint at different pressures and time[44]: (a) 0.2 MPa, 1 min; (b) 0.2 MPa, 1 h; (c) 2 MPa, 2 h

头，保温到960 min时孔洞消失；当300 ℃保温960 min时，焊点仅由Cu_3Sn组成，但仍存在孔洞[45]。将Cu/Sn(0.8 μm)/Cu结构于320 ℃和0.6 MPa压力下保温30 min，成功制备了全Cu_3Sn焊点；当250 ℃且压力增加为4~10 MPa时，保温30 min时接头由无缺陷的全Cu_3Sn组成[46]。

此外，在200 ℃和0.04 MPa压力下将Ag/In(3~8 μm)/Ag互连结构保温3600 s后获得了完全由γ

(Ag_2In)/$AgIn_2$/γ(Ag_2In)组成的接头；当温度升高至225 ℃，保温时间减少为400 s后其接头由γ(Ag_2In)和$AgIn_2$组成；当保温时间为1200 s时，其接头仅由γ(Ag_2In)组成[47]。在503 K和10 MPa压力下，Cu/Sn(2 mm)/Ag(1 mm)/Sn(2 mm)/Si(Cu)结构在氮气中保温1800 s，获得由Cu_6Sn_5+Ag_3Sn+Ag_4Sn组成的接头，且Cu_6Sn_5和Ag-Sn金属间化合物层间存在大量连续孔洞；523 K时开始出现Cu_3Sn，接头由Cu_6Sn_5+Cu_3Sn+Ag_3Sn+Ag_4Sn组成，界面仍存在孔洞；当温度达到573 K时，Cu_6Sn_5相消失，只剩下Cu_3Sn+Ag_3Sn+Ag_4Sn层[48]。Ni颗粒可细化晶粒，同时诱导弥散的非界面形核，有效防止晶粒合并现象，如采用Sn-Ni焊料中间层在260 ℃键合45 min后，形成了以(Cu, Ni)$_6Sn_5$为主和少量Cu_3Sn组成的全IMC焊点(见图4)[49]。Ni/Sn(2 μm)/Ni结构在360 ℃和300 ℃下分别保温5 min和20 min后都制备了Ni/Ni_3Sn/Ni_3Sn_2/Ni_3Sn/Ni接头，且在接头中心线形成了大小不一的气孔[50]。低固液互扩散键合制备IMC熔点较高，可以达到低温键合、高温服役的效果[44]。虽然低固液互扩散键合制备全IMC具有成本低、机械强度高等优点，但其连接层厚度必须要控制在合适的范围，过厚或太薄都会影响焊点可靠性。

1.3　瞬态液相键合制备全IMC焊点

瞬态液相(TLP)键合是采用低熔点的中间层和高熔点的金属基板，通过扩散生成具有高熔点金属化合物焊点的技术，获得的焊点具有较好的高温热可靠性。在235 ℃保温150 min时Cu-Sn TLP焊点完全由Cu_6Sn_5+Cu_3Sn组成，在250 ℃保温120 min时焊点中Sn被完全消耗；而在265 ℃下保温60 min后Cu-Sn焊点中Sn被完全消耗，但Cu_3Sn层内部出现了许多孔洞(见图5)[51]。采用低温瞬态液相法(LTTLP)将Cu/Sn(8 μm)/Cu结构置于300 ℃和0.1 MPa压力下，保温60 min后Sn已被完全消耗，接头由Cu_6Sn_5+Cu_3Sn组成，150 min时焊点完全由Cu_3Sn组成[52]。不同厚度Sn层(3 μm、3.5 μm、5 μm)的Cu-Sn TLP焊点在260 ℃保温30 min后都能完全转化为Cu_3Sn(见图6)[53]。纯铜基板和镀铜基板焊点中Sn层(2.5 μm)在240 ℃键合15 min后均完全转变为Cu_6Sn_5+Cu_3Sn；290 ℃相同保温时间内镀铜基板的接头完全转变Cu_3Sn焊点[54]。将具有微孔的铜片(1 mm厚)浸渍到液体锡制备成复合焊料从而作为中间层，在300 ℃和0.6 MPa压力条件下，保温2 min后接头完全由Cu_3Sn+Cu_6Sn_5组成；当保温15 min时获得了单一的Cu_3Sn接头(见图7)[55]。将Ni/Sn(40 μm)/Cu互连结构在260 ℃条件下，保温120 min后接头完全由(Cu, Ni)$_6Sn_5$+Cu_3Sn组成；基板两侧均形成了(Cu, Ni)$_6Sn_5$，镍侧向铜侧其形貌依次为小颗粒状、针状和扇贝状[56]。在300 ℃保温2 h后，Cu-Sn TLP接头完全转化为Cu_6Sn_5+Cu_3Sn，Sn-Ni TLP接头完全转化为Ni_3Sn_4，但接头中出现富Ni层[57]。在280 ℃和50 kN压力下的N_2气氛中保温20 min后，Cu/Sn(3 μm)/Cu和Ni/Sn(3 μm)/Ni互连结构分别转化为Cu_6Sn_5+Cu_3Sn接头和Ni_3Sn_4+Ni_3Sn_2接头，Ni_3Sn_4的形成导致体积大量收缩，在Ni-Sn TLP焊点中部形成小孔洞[58]。由于金属间化合物的形成只发生在高熔点金属和低熔点金属之间的界面处[59]，因此通过向低熔点金属中间层中加入高熔点金属颗粒或中间层以诱导IMC在金属颗粒或中间层中形成，可缩短TLP键合的时间。如采用SAC305+10%Ag颗粒作为中间层，在300 ℃无压保温2 h后制备了无孔洞的Cu/Cu_6Sn_5/Cu_3Sn/Ag_3Sn/Cu接头[60]。Cu/Sn/Cu互连结构中引入Ag中间层，在300 ℃和0.3 MPa压力下保温420 min后制备了由Cu_3Sn+Ag_3Sn+Ag_4Sn组成的TLP接头；350 ℃老化

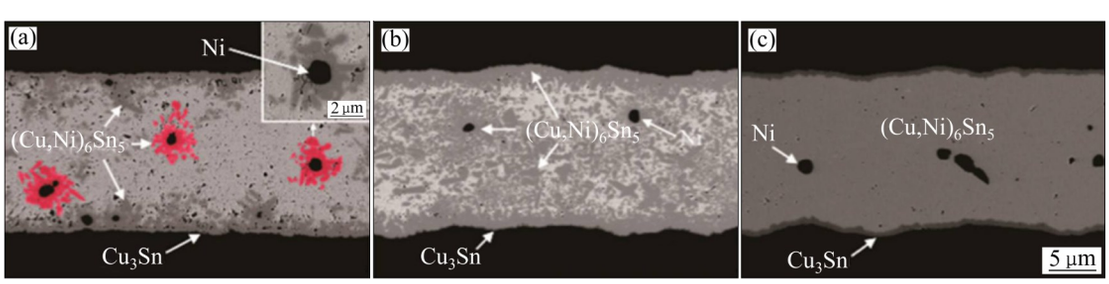

图4　260 ℃键合不同时间下Sn-Ni体系SLID接头的SEM像[49]

Fig. 4　SEM images of Sn-Ni system SLID joint at 260 ℃ for different time[49]: (a) 15 min; (b) 30 min; (c) 45 min

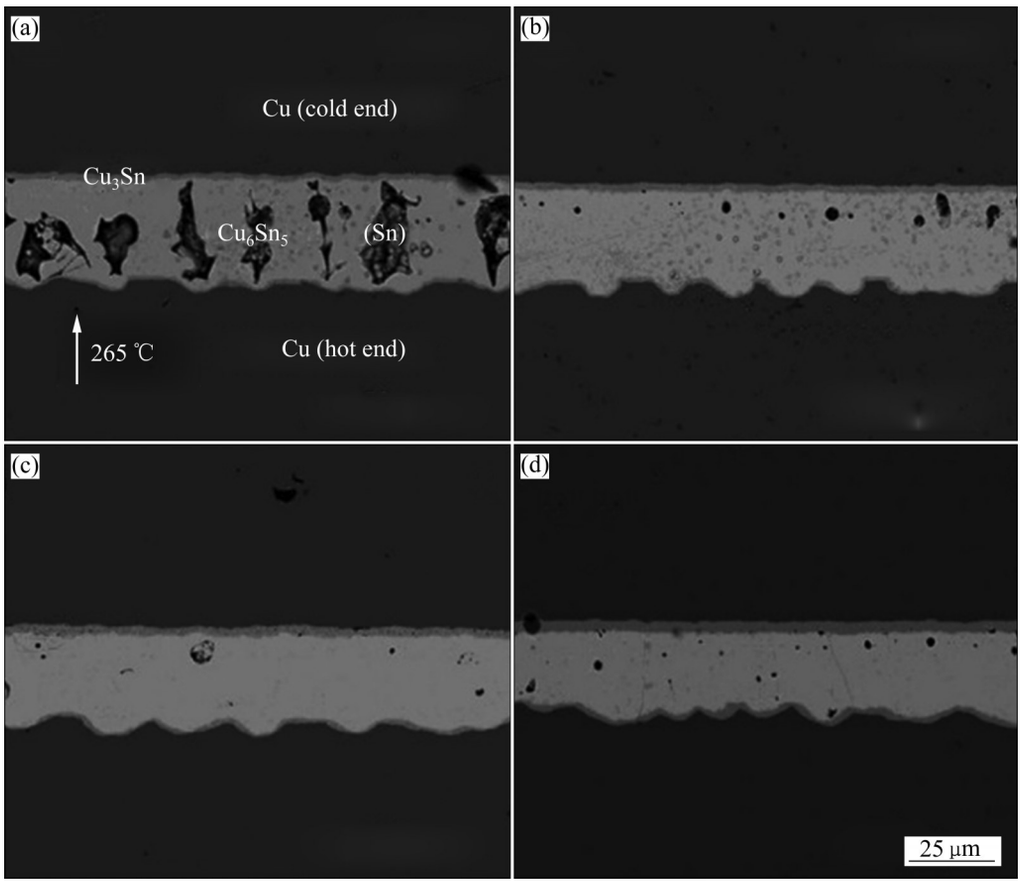

图5 265 ℃保温不同时间下Cu-Sn焊点截面的SEM像[51]

Fig. 5 Sectional SEM images of Cu-Sn solder joints held at 265 ℃ for different time[51]: (a) 30 min; (b) 60 min; (c) 90 min; (d) 150 min

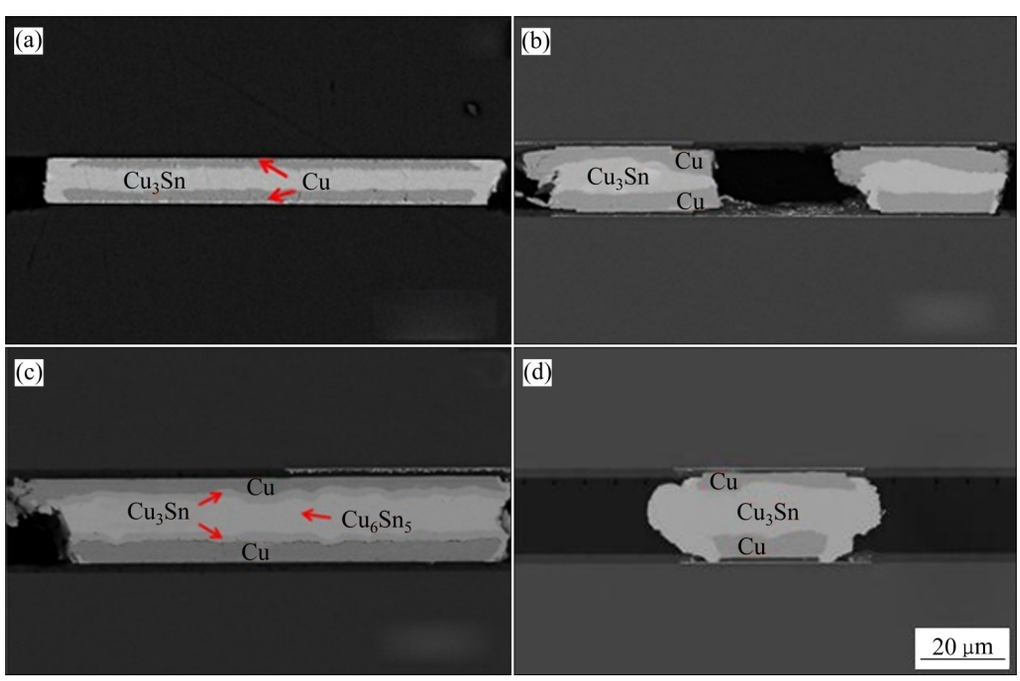

图6 不同Sn厚度键合界面的SEM像[53]

Fig. 6 SEM images of bonding interfaces with different Sn thicknesses[53]: (a) 3 μm; (b) 3.5 μm; (c) 4 μm; (d) 5 μm

24 h 后，Ag_3Sn 完全转变为 Ag(Sn)固溶体，Cu-Sn IMC 层由 Cu_3Sn+$Cu_{41}Sn_{11}$ 组成；时效 480 h 后，Cu_3Sn+Cu→$Cu_{41}Sn_{11}$ 的转变结束，当时效时间增加到 960 h 后 Cu(Sn)固溶体在许多区域与 Ag(Sn)固溶体密切接触(见图 8)[61]。

1.4　无压瞬态液相键合制备全 IMC 焊点

TLP 键合过程中，长时间地施加压力对封装体产生一定的危害，但不施加压力接头中间则会形成空隙，并严重降低其力学性能，因而无压瞬态液相烧结(TLPS)应运而生。如采用 30Ni-70Sn 作为中间层，在 340 ℃和 240 min 无压条件下制备了由 Ni_3Sn_4 和残余 Ni 颗粒组成接头(见图 9)；在 500 ℃保温 36 h 后，残余的 Ni 颗粒逐渐溶解，形成以 Ni_3Sn_2 为主的稳定结构，但由于 Ni_3Sn_2 的形成导致体积收缩而形成大量的孔洞[62]。将 Cu、Ni、

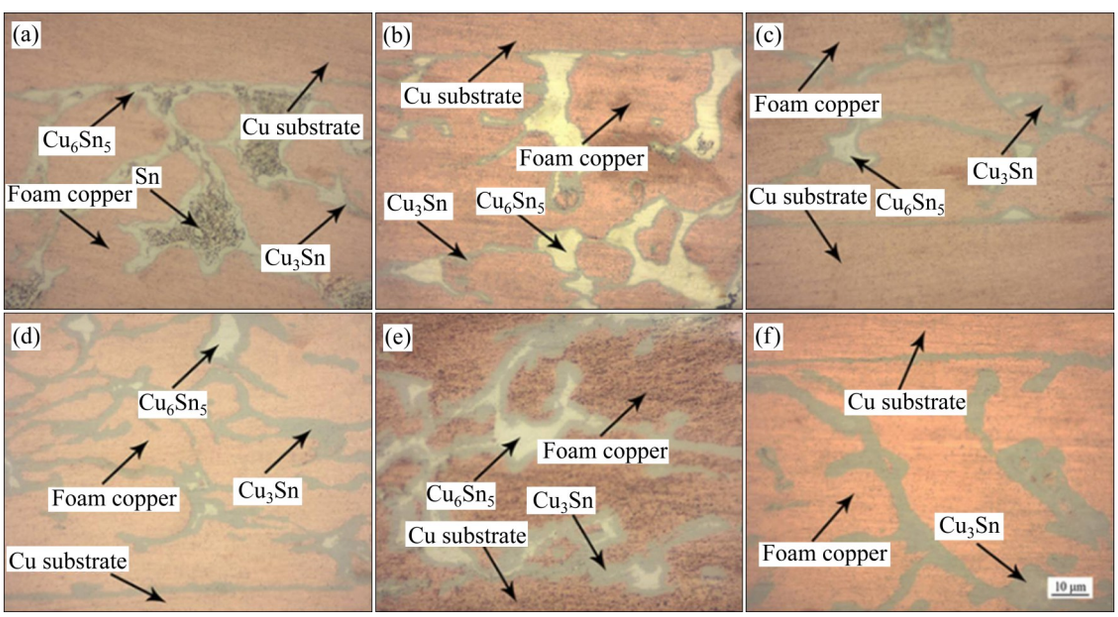

图 7　不同保温时间下 Cu/Cu_3Sn-Cu/Cu 复合材料接头的 SEM 像[55]

Fig. 7　SEM images of Cu/Cu_3Sn-Cu/Cu composite joints with different holding time[55]: (a) 30 s; (b) 2 min; (c) 4 min; (d) 6 min; (e) 8 min; (f) 15 min

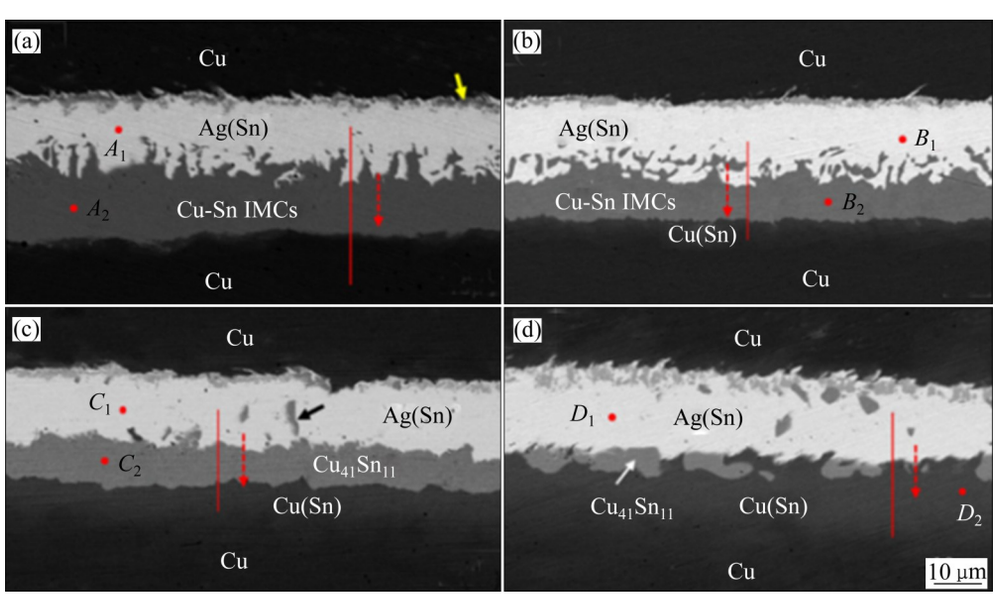

图 8　Cu/Sn/Ag 接头在 350 ℃不同时效时间下时效界面的 SEM 像[61]

Fig. 8　SEM images of interface of Cu/Sn/Ag joints aging at 350 ℃ for different time[61]: (a) 24 h; (b) 120 h; (C) 480 h; (d) 960 h

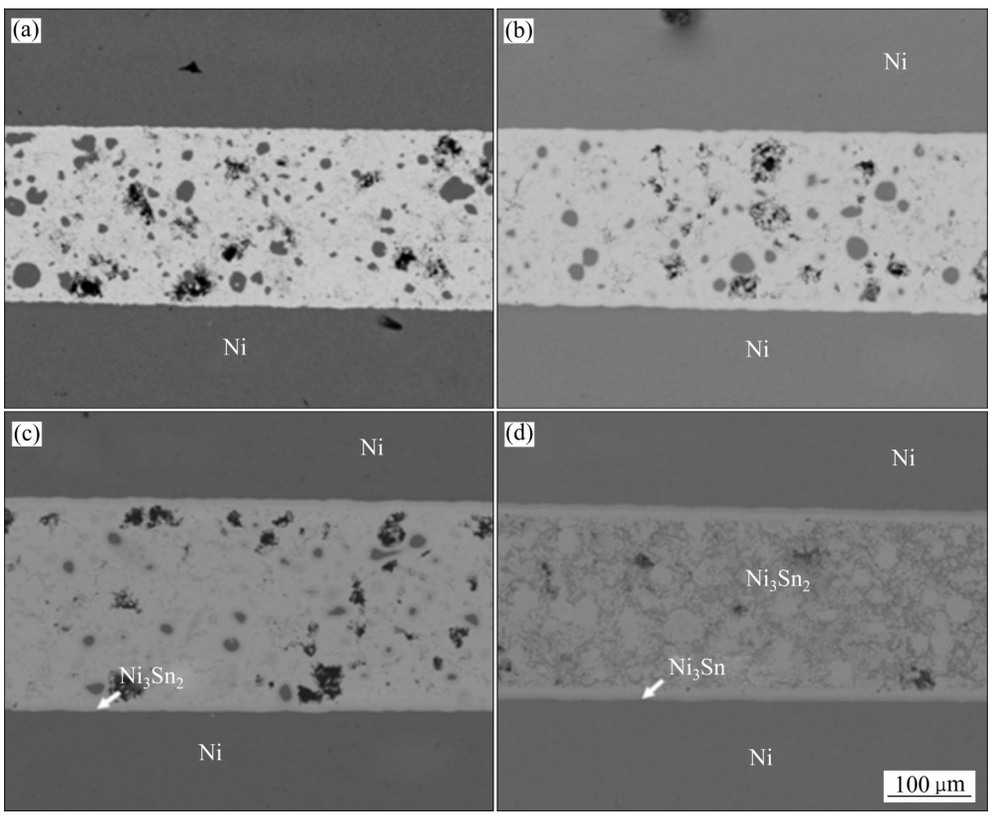

图9 不同时效条件下焊点断面的SEM像[62]

Fig. 9 Sectional SEM images of solder joints with different aging conditions[62]: (a) Original joint; (b) 350 ℃, 100 h; (c) 500 ℃, 6 h; (d) 500 ℃, 100 h

SAC305颗粒的混合膏体作为中间层在260 ℃下保温3 h后，接头由(Cu, Ni)$_6$Sn$_5$+Cu$_3$Sn+Ag$_3$Sn组成，但存在较多孔洞[63]。在220 ℃下无压键合60 min制备Sn-Bi接头，接头由Cu$_6$Sn$_5$+Cu$_3$Sn+Bi+Cu组成；键合90 min时接头中只存在Cu$_3$Sn+Bi[64]。将SAC305颗粒(粒径3 μm)和Cu颗粒(粒径10 μm)的混合物作为中间层，在250 ℃无压保温1 min制备了由Cu+Cu$_6$Sn$_5$+Cu$_3$Sn组成的接头，热时效1000 h后Cu$_6$Sn$_5$相完全转变为Cu$_3$Sn，但Cu$_3$Sn和Cu颗粒之间的亚微米孔洞数量随时效时间增加而增加[65]。还有学者采用含有微晶Cu颗粒(粒径6.2 μm)的Sn涂层(50 μm厚)作为中间层，300 ℃无压保温30 s获得了Cu颗粒分散的Cu$_3$Sn焊点，该接头具有优异的热稳定性能[66]。TLPS主要用于Cu-Ni、Cu-Sn、Sn-Ag体系等全IMC接头的制备，不仅解决了压力对封装体的影响，缩短了键合时间，而且获得具有更高力学可靠性的接头。目前，该技术已广泛应用于电子元器件的低温焊接领域[67−68]。

1.5 其他方法制备全IMC焊点

传统低温烧结、SLID和TLP等方法由于制备全IMC焊点需要的时间长达数小时，键合时间过长会产生额外的热应力，从而严重影响封装系统的可靠性。基于此，国内外学者通过采用感应加热[69−70]、超声辅助TLP[72−75]、电流辅助键合[78]等方法短时间来制备全IMC焊点。如采用感应加热将Cu/Sn(10 μm)/Cu结构在0.01 MPa压力下保温，220 s后接头由Cu$_6$Sn$_5$+Cu$_3$Sn组成，270s时其接头为Cu/Cu$_3$Sn/Cu(见图10)[69]。Cu/Sn/Cu结构在225 kHz高频感应加热3 min成功制备了上下端均为Cu$_{43}$Sn$_7$、中间为Cu$_3$Sn+Cu$_{43}$Sn$_7$的接头，但IMC接头存在大量孔洞；当加热时间增加到4 min时，其接头由Cu$_{43}$Sn$_7$+Cu$_{19}$Sn组成，且无孔洞存在；当频率提高至300 kHz，加热2 min后接头同样由Cu$_{43}$Sn$_7$+Cu$_{19}$Sn组成(见图11)[70]。相对于电磁感应加热，超声辅助TLP键合具有更加明显的优势，如在300 ℃对其Cu/Sn(35 μm)/Cu结构超声处理60 s后可以获得完整的Cu$_3$Sn结构[71]。SiC/Sn-0.7Cu/Cu

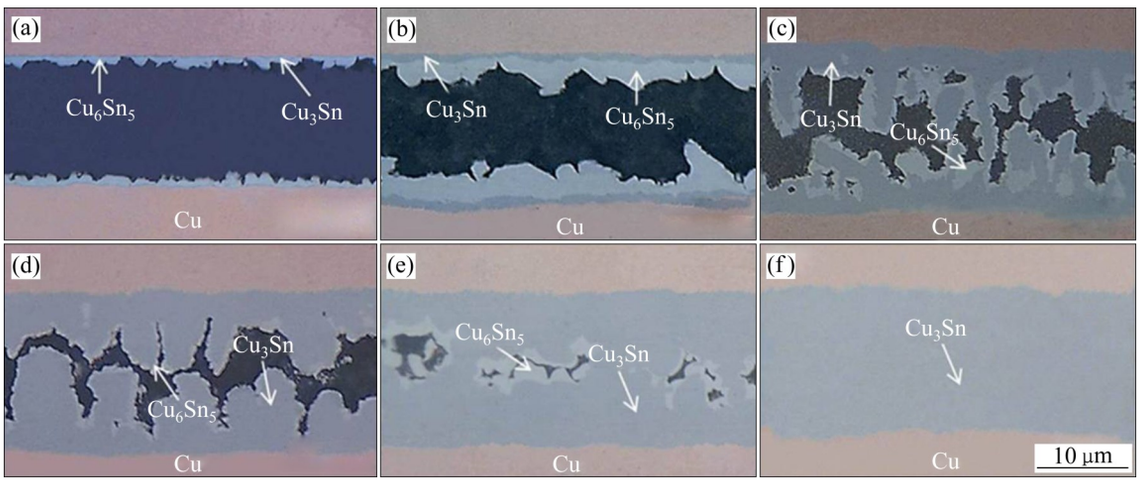

图 10　不同感应加热时间下 Cu/Sn/Cu 界面的 SEM 像[69]

Fig. 10　SEM images of interface of Cu/Sn/Cu for different induction heating time[69]: (a) 20 s; (b) 35 s; (c) 55 s; (d) 100 s; (e) 220 s; (f) 270 s

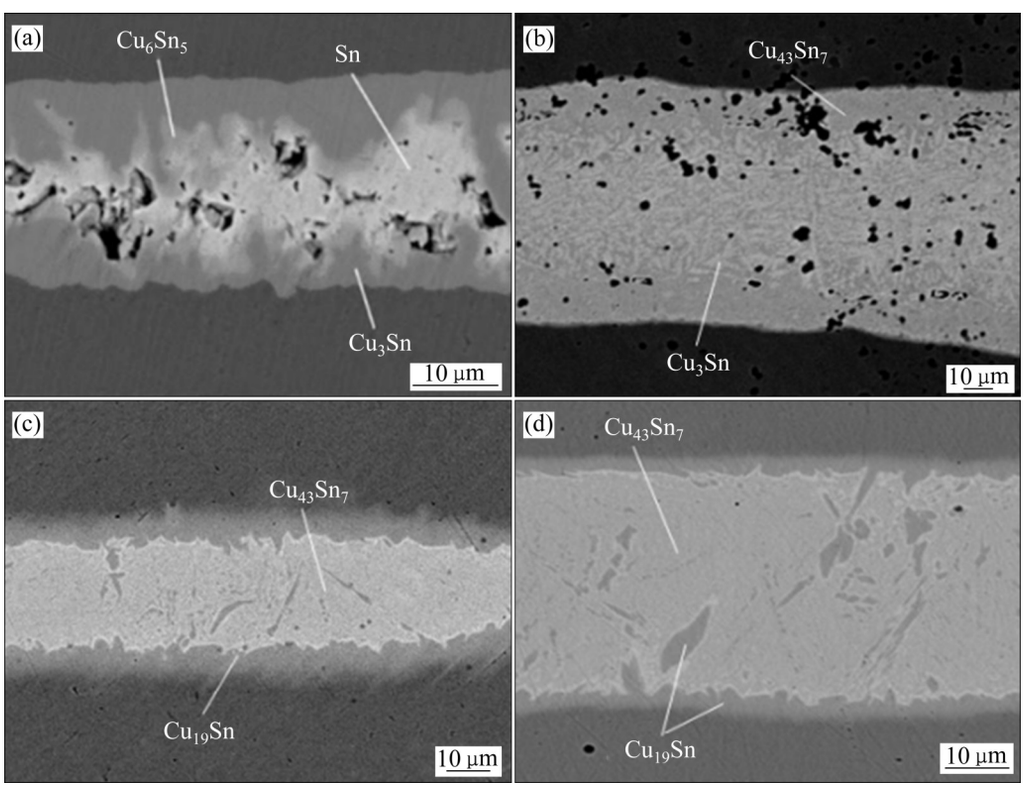

图 11　不同磁场频率和加热时间焊点的 SEM 像[70]

Fig. 11　SEM images of solder joints with different magnetic field frequencies and heating time[70]: (a) 225 kHz, 2 min; (b) 225 kHz, 3 min; (c) 225 kHz, 4 min; (d) 300 kHz, 2 min

结构在 250 ℃和 0.3 MPa 压力下，超声处理 10 s 后焊点由 Cu_3Sn 和 $(Cu, Ni)_6Sn_5$ 组成(见图 12)[72]。Cu/Sn(25 μm)/Cu 结构在 277~297 ℃超声处理 2~3 s 后获得了由均匀的 Cu_6Sn_5 组成的接头；超声处理 4 s 时焊点由 Cu_6Sn_5→Cu_6Sn_5+Cu_3Sn 转变[73]。电流通过时，金属离子会沿导体产生质量的输运，而电迁移、点缺陷的产生和缺陷迁移率能增强质量传输[76−77]。因此，有学者将 Cu/Sn(30 μm)/Cu 结构在 0.08 MPa 压力和 1.3×10^4 A/cm^2 电流密度下通电 200 ms 后，成功制备了 Cu_6Sn_5+Cu_3Sn 焊点，但界

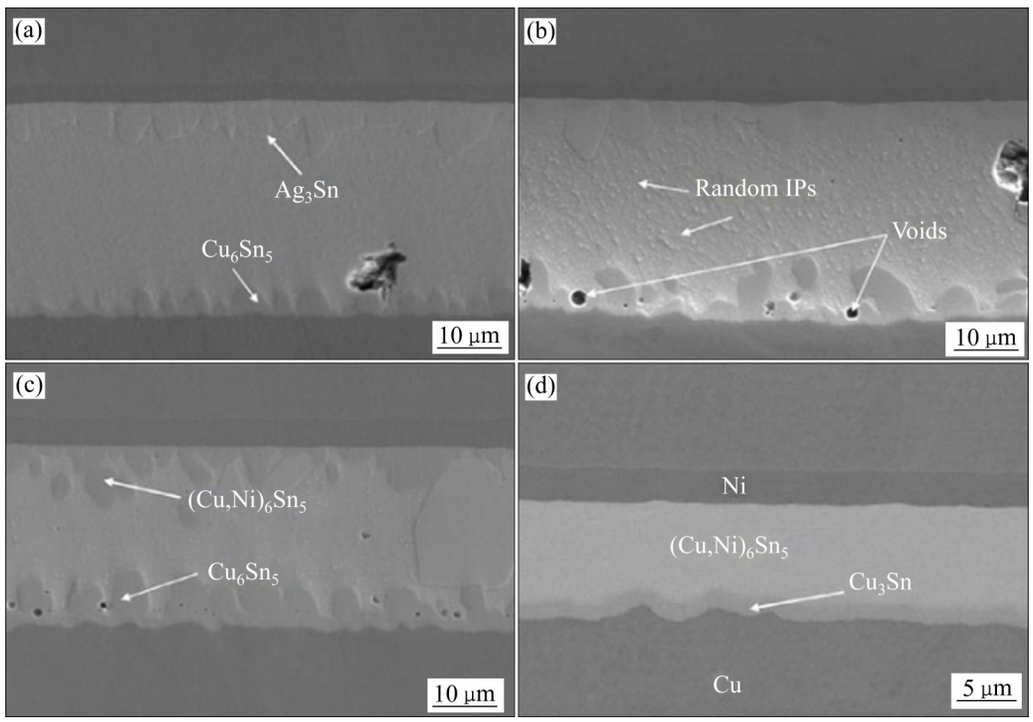

图12 不同超声辅助键合时间的芯片/Sn0.7Cu/Cu焊点横截面的SEM像[72]

Fig. 12 SEM images of cross section of chip/Sn0.7Cu/Cu solder joints with different ultrasonic assisted bonding time[72]: (a) 0 s; (b) 3 s; (c) 5 s; (d) 10 s

面仍存在少量孔洞；当电流增加到1.4×10^4 A/cm^{2}或1.5×10^4 A/cm^{2}时，在相同时间内焊点只存在$Cu_3Sn+Cu_{41}Sn_{11}$，且电流辅助键合接头成型良好[78]。采用热压缩键合方法将Cu/SAC105(20 μm)/Cu结构在450 ℃和0.016 MPa压力条件下保温9 s就获得了$Cu_3Sn+Cu_6Sn_5$接头，当保温时间增加至9.9 s时，接头只存在Cu_3Sn[79]。总之，感应加热、超声辅助TLP、电流辅助键合等方法制备全IMC焊点的研究主要集中在Cu-Sn体系，对其他体系的研究较少。

综上所述，对于低温烧结法，烧结过程中很容易产生孔洞和裂纹，接头键合时间长。而固液互扩散键合对其连接层厚度必须要控制在合适的范围，过厚或太薄都会影响焊点可靠性；同样也存在键合时间过程长、焊接压力高等缺点。虽然对于TLP/TLPS方法在一定程度上解决了低温烧结和SLID的问题，但对于现有生产情况来看，仍然存在着焊接时间长，接头时有孔洞。而对于感应加热、超声辅助TLP、电流辅助键合等虽然极大地缩短了焊接时间，但对于接头孔洞的问题仍未解决且大多数方法仍处于实验室研究中，应用在实际生产过程中仍然有一定的距离。

2 不同焊料体系制备全IMC焊点的研究进展

不同的焊料体系，不同工艺条件所制备的接头性能存在较大差异。目前，用于制备全IMC焊点的互连材料主要有Cu-Sn[80−83]、Cu-In[84−87]、Sn-Ag[60, 88]、Sn-Ni[89−91]等焊料体系。

2.1 Cu-Sn体系制备全IMC焊点的研究

锡熔点低(232 ℃)，在Cu中相对较高的溶解度，加之Cu-Sn金属间化合物优于传统锡基钎料的强度和抗蠕变性能，故Cu-Sn体系已广泛应用于制备全IMC焊点。Cu-Sn体系一般采用低温烧结法、固液互扩散键合法、瞬态液相法和超声辅助瞬态液相法形成Cu_6Sn_5和Cu_3Sn焊点，基于较好的接头强度及较低的成本，Cu-Sn体系制备全IMC焊点被应用在高温封装领域中。如通过烧结$Cu_{10}Sn_3$纳米颗粒制备了全$Cu_{10}Sn_3$接头，烧结温度为260 ℃、

280 ℃和300 ℃时，接头的平均抗剪强度分别为5.1、17.2和26.8 MPa[39]。Sn-0.7Cu焊料作为中间层，在300 ℃和0.2 MPa压力下固液互扩散键合1 min时，接头由Sn+Cu_6Sn_5+Cu_3Sn组成，剪切强度为35 MPa；当保温1 h后接头完全由Cu_6Sn_5+Cu_3Sn组成，抗剪强度明显降低(10 MPa)；而当压力和保温时间分别增加到2 MPa和2 h时，接头由Cu_3Sn组成，抗剪强度约为55 MPa[44]。

Cu/Sn/Cu结构在235~265 ℃采用瞬态液相法可制备Cu_6Sn_5+Cu_3Sn焊点，其剪强度随温度和时间的增加而逐渐增大，达8.5~24.2 MPa[51]。将具有微孔的铜片(1 mm厚)浸渍到液体锡制备成复合焊料作为中间层，在300 ℃和0.6 MPa压力条件下保温15 min后获得了单一的Cu_3Sn接头，其接头剪切强度约为155 MPa[55]。Cu/Sn(5 μm)/Cu结构在255 ℃和25 MPa压力下保温60 min，瞬态液相法制备了Cu_6Sn_5+Cu_3Sn接头，平均剪切强度达90~95 MPa[92]。将经过氧化物弥散强化的铜棒及纯Sn作为中间层，在400 ℃下瞬态液相键合保温4 h后制备了$Cu_{41}Sn_{11}$接头，接头弯曲强度达到300 MPa，但韧性较低(5 MPa·$m^{1/2}$)；向中间层中加入Cu颗粒并进行热处理，其接头弯曲强度和韧性增加了30%(400 MPa、7 MPa·$m^{1/2}$)；随着时效时间的增加，接头IMC向Cu固溶体转变，其接头弯曲强度降低至200 MPa，但韧性增加至13 MPa·$m^{1/2}$ [93]。Cu/Sn(50 μm)/Cu互连结构，在300 ℃下无压保温30 s后制备了Cu_3Sn接头, 未时效时其抗剪强度为24.2 MPa，300 ℃空气时效200 h后剪切强度变化不大[66]。

在0.6 MPa压力下超声处理4 s后，Si/Sn(20 μm)/Si互连结构形成了完全由Cu_3Sn组成的接头，其抗剪强度为65.8 MPa[81]。Cu/Sn(50 μm)/Cu互连结构在250 ℃和0.4 MPa压力下，超声处理30 s后制备了Cu_6Sn_5+Cu_3Sn接头，其接头的剪切强度为60 MPa[83]。Cu/Sn(20 μm)/Cu互连结构在250 ℃和0.5 MPa压力下，超声处理4 s制备了Cu_6Sn_5+Cu_3Sn焊点，其抗剪强度达到60 MPa；超声处理8 s后焊点完全由Cu_3Sn组成，其剪切强度为65 MPa[94]。含40%铜的锡膏作为中间层，在250 ℃和0.25 MPa压力下超声处理10 s后获得了全Cu_3Sn接头，其常温下剪切强度为49.96 MPa，350 ℃高温下剪切强度为46.54 MPa[95]。

2.2　Cu-In体系制备全IMC焊点的研究

与广泛研究的Cu-Sn互连相比，In具有较低的熔化温度(156.6 ℃)和作为金属化层的良好兼容性，其互连成键温度低，成键性能更好，已广泛应用于制备全IMC焊点。Cu-In体系大量应用于SLID和TLP键合，一般形成Cu_7In_3+Cu_2In焊点，且Cu_7In_3的剪切性能比Cu_2In的差。如Cu/In/Cu互连结构，260 ℃保温360 min固液互扩散键合制备了$Cu_{11}In_9$+Cu_2In接头，由于界面存在Kirkendall孔洞故其剪切强度只有9.07 MPa；在360 ℃保温40 min时，焊点中只存在Cu_2In，其剪切强度升至13.65 MPa；与保温360 min后获得的Cu_7In_3焊点(12.31 MPa)相比具有更好的力学性能[30]。

200 ℃下采用瞬态液相键合300 s制备的Cu-In焊点，经过300 ℃高温老化后，焊点完全由Cu_7In_3组成，其剪切强度在23~25 MPa之间，断裂发生在Si芯片上[85]。In-45Cu作为中间层，在260 ℃采用瞬态液相键合30 min成功制备了$Cu_{11}In_9$+Cu颗粒的接头，其接头强度达到最大值(16.34 MPa)；当时间增加到60 min时，接头中只存在Cu_2In+$Cu_{11}In_9$，但$Cu_{11}In_9$和Cu_2In界面出现大量裂纹，从而导致其力学性能下降[96]。采用In-50Ag作为中间层，在260 ℃和1 MPa压力下瞬态液相键合制备了全IMC焊点，$(Ag, Cu)_2In$相随着键合时间的延长而转变为Cu_2In相，保温30 min后接头只存在Cu_2In+Ag_2In(见图13)；如图14所示，TLP焊点的孔隙率呈先急剧下降后缓慢上升的趋势；当键合时间延长到30 min时，焊点的孔隙率最小(1.85%)，剪切强度变化趋势则相反(见图14(b))[97]。尽管其Cu-In体系键合温度相对Cu-Sn而言更低，但键合过程中由于相变极容易产生裂纹和孔洞，加之In属于稀有金属，故Cu-In体系在高温封装领域中难以得到广泛应用，主要应用于一些特殊环境中耐高温焊点的制备。

2.3　Sn-Ag体系制备全IMC焊点的研究

Ag具有优越的导电性和导热性，加之Ag_3Sn比Cu-Sn和Ni-Sn金属间化合物具有更好的断裂韧性，故Ag_3Sn化合物作为全IMC的理想选择，主要采用SILD和TLP法制备Sn-Ag体系全IMC焊点。如Cu/Sn/Ag/Sn/Cu互连结构分别在250 ℃和300 ℃下加压10 MPa时，固液互扩散键合接头都由Cu_3Sn和Ag_4Sn组成，其剪切强度达到最大值(120 MPa)

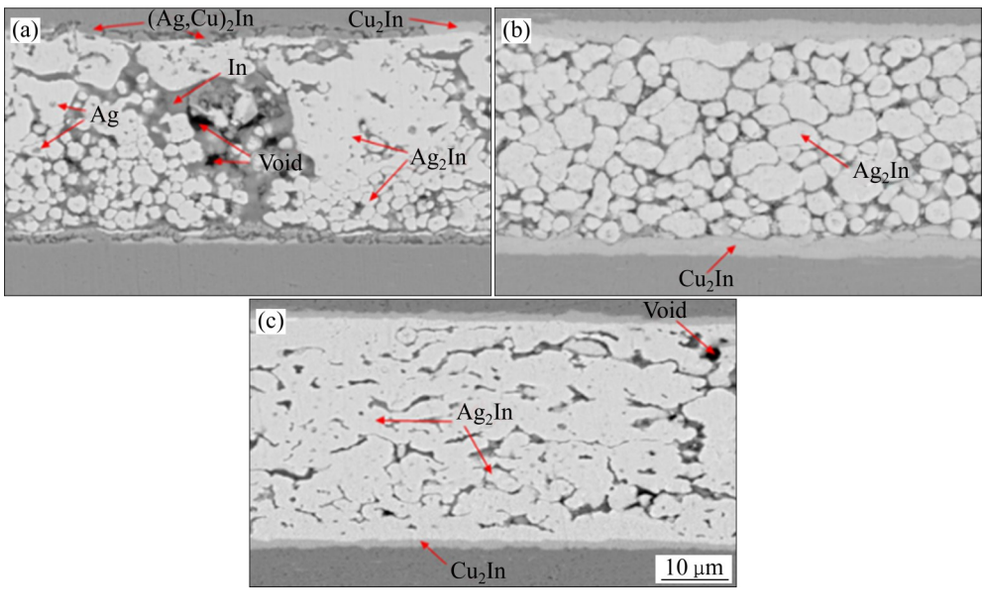

图 13 不同键合时间下 Cu/In-50Ag/Cu 焊点的微观结构[97]

Fig. 13 Microstructures of Cu/In-50Ag/Cu solder joints at different bonding time[79]: (a) 0.5 min; (b) 30 min; (c) 60 min

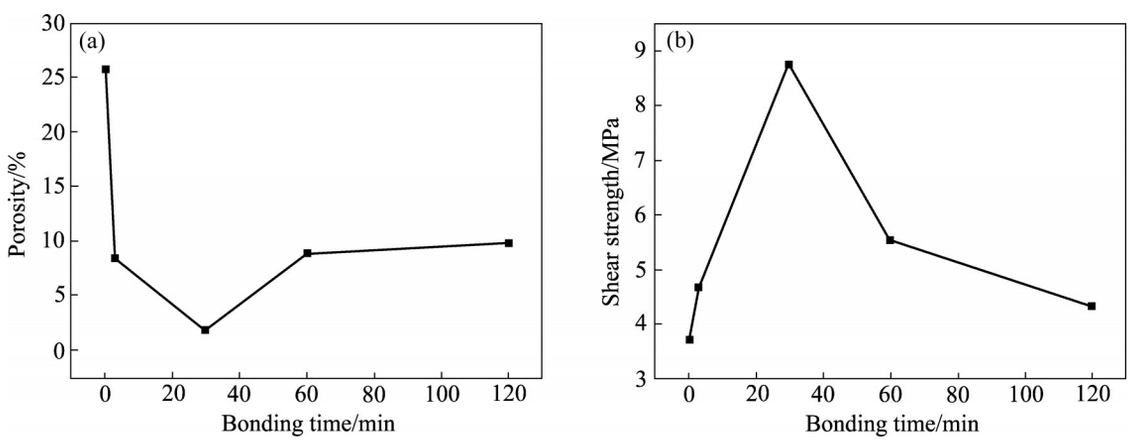

图 14 不同键合时间下 TLP 焊点的孔隙率和剪切强度[97]

Fig. 14 Porosity(a) and shear strength(b) of TLP solder joints at different bonding time[97]

并保持不变(见图 15)[48]。采用 Sn70Ag 作为中间层，在 260 ℃下保温 10 min，瞬态液相键合焊点由 Cu_6Sn_5+Cu_3Sn+Ag_3Sn 组成，其剪切强度为 39.5 MPa[98]。

Ag/Sn/Cu 互连结构在 300 ℃保温 420 min，制备了 Ag+Ag_3Sn+Cu_3Sn 低温瞬态液相键合接头，其剪切强度为 60.2 MPa，Cu_6Sn_5/Ag_3Sn 界面的键合强度比 Cu_3Sn/Ag_3Sn 界面弱，裂纹产生于界面空隙处(见图 16)；Cu_3Sn+Cu_6Sn_5+Ag_3Sn 焊点组成时裂纹主要沿 Cu_6Sn_5/Ag_3Sn 界面裂纹扩展，而 Cu_3Sn+Ag_3Sn 焊点组成时裂纹只穿过 Cu_3Sn 层[99]。Ag/Sn(10 μm)/Ag 互连结构 250 ℃下瞬态液相键合后获得了全 IMC 接头，接头界面存在较多孔洞，其接头强度大约为 31 MPa；当在 Ag 基板上镀一层薄 Cu 膜，引入第二相 Cu_6Sn_5 颗粒，有效地填充了沿 Ag_3Sn 晶界分布的微孔，在 350 ℃下 Ag (Cu)/Sn/Ag 全 IMC 接头的抗剪强度最高可达 40 MPa 以上；当基板替换为 Cu 基板之后，在 350 ℃下 Cu/Sn/Ag 全 IMC 接头的抗剪强度最高可达 48 MPa[100]。Ag/Sn(10 μm)/Ag 互连结构在 300 ℃和 0.5 MPa 压力下，保温 90 min 后成功制备了 Ag_3Sn 接头，其剪切强度最高为 50.3 MPa；当加入 Cu 中间层后，在 300 ℃和 0.3 MPa 压力下，保温 300 min 接头由 Ag_3Sn+Cu_3Sn 组成，其剪切强度达到 35 MPa，断裂路径不仅沿 IMCs 延

伸，还贯穿 Cu 层(见图 17)，但焊点的塑性得到了提高[101]。在 250 ℃和 5 MPa 压力下保温 10 min 后制备了 Ag/Sn/Cu 瞬态液相键合接头，200 ℃热老化 500 h 后，其接头组织由 Ag/Ag_3Sn/Cu_6Sn_5/Cu 转变为 Ag/(Ag)/ (ζ-Ag)/ Cu_3Sn/Cu，老化前后接头平均剪切强度分别为 49.57 MPa 和 50.03 MPa[102]。有学者对 Cu/Sn/Ag 瞬态液相键合接头在 350 ℃进行时效，发现随着时效时间的增加，抗剪强度先降低然后逐渐增加(见图 18)，以致于当时效为 960 h 时 Cu/Sn/Ag TLP 接头仍保持较高的强度(44.6 MPa)[61]。虽然 Sn-Ag 体系焊点性能良好，但收缩孔是 Ag-Sn 瞬态液相键合焊点中常见的缺陷，加之贵金属 Ag 含量较高，因此 Sn-Ag 体系在实际生产过程中有一定的局限性。

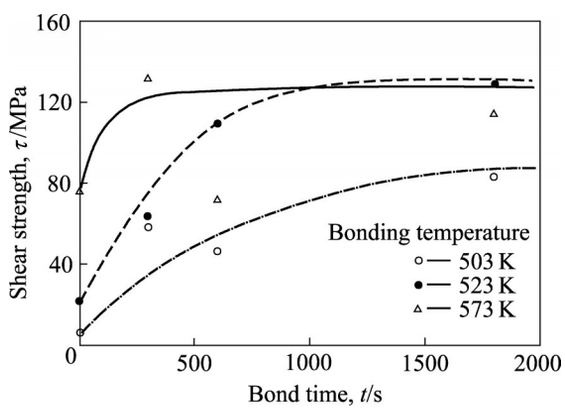

图 15　在 10 MPa 压力不同键合温度下接头的抗剪强度[48]

Fig. 15　Shear strengths of joints at 10 MPa pressure at different bonding temperatures[48]

2.4　Sn-Ni 体系制备全 IMC 焊点的研究

一般情况下，Ni_3Sn_4 是 Sn/Ni 体系键合后的唯一反应产物，且 Ni_3Sn_4 熔点(794 ℃)接近电子封装领域的最高温度。其次，在 Sn 和 Ni_3Sn_4 中，Ni 原子的扩散速度非常缓慢，这可以延缓 Ni_3Sn_4 向 Ni_3Sn_2/Ni_3Sn 的转变，延长电子器件的使用寿命，因此 Sn-Ni 体系在电子封装备受关注。如 Ni(P)/Sn/Ni(P)互连结构，TLP 键合后界面只形成 Ni_3Sn_4，当键合时间 2 h 以上时 TLP 焊点中还发现了 Ni_2SnP、Ni_3P 和间隙 Sn[103]。Ni/Sn(30 μm)/Cu 互连结构在 260 ℃下保温 120 min 后可获得完全由(Cu, Ni)$_6Sn_5$ 和 Cu_3Sn 组成的 TLP 接头，其剪切强度为(49.8±0.3) MPa，剪切断裂倾向于发生在(Cu, Ni)$_6Sn_5$ 晶粒粗大的圆形区域[104]。Ni/Sn(30 μm)/Cu 互连结构在 260 ℃、300 ℃和 340 ℃下保温 120 min 后，成功制备了(Cu, Ni)$_6Sn_5$ 和 Cu_3Sn 全 IMC 瞬态液相键合接头，其抗剪强度分别为 49.8 MPa、50.3 MPa 和 42.7 MPa；260 ℃和 300 ℃的 TLP 接头断裂发生在粗圆状颗粒区，340 ℃的 TLP 接头断裂发生在粗棱柱状颗粒区[105]。

超声辅助 TLP 制备的 Sn-Ni 焊点在 300 ℃下时

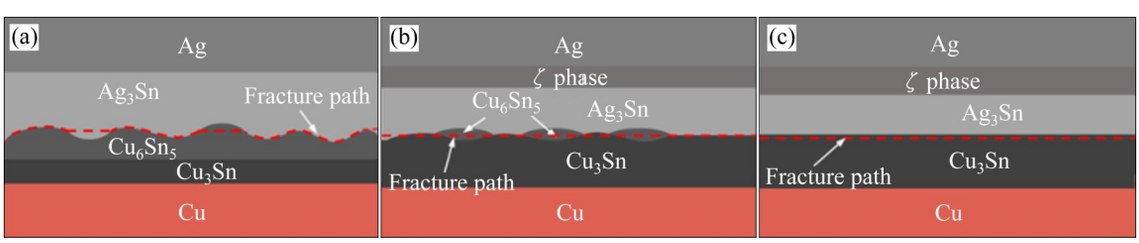

图 16　不同微观结构的焊点断裂模型[99]

Fig. 16　Fracture models of solder joints with different microstructures[99]

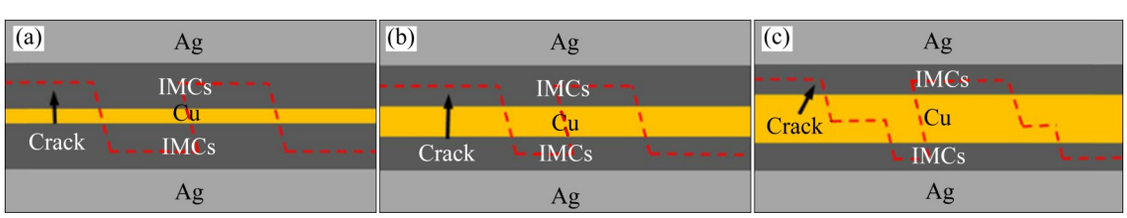

图 17　不同 Sn/Cu/Sn 预成形层间连接 TLP 焊点的断裂模型[101]

Fig. 17　Fracture models for different typical TLP joints bonded by preformed Sn/Cu/Sn interlayer[101]: (a) I-cracks uniformly propagate through thin residual Cu layer; (b) II-cracks randomly propagate through thicker residual Cu layer; (c) III-cracks randomly propagate through even within much thicker residual Cu layer

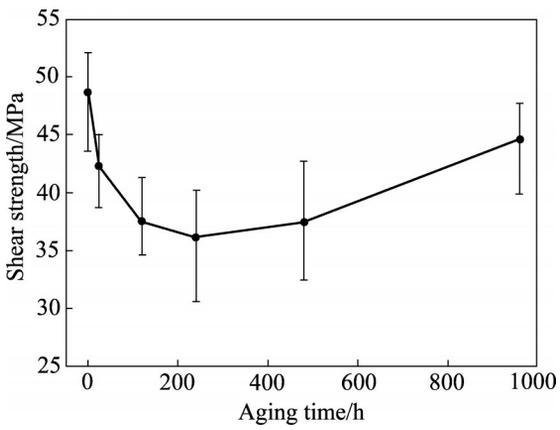

图18 接头剪切强度随老化时间的变化关系[61]

Fig. 18 Relationship between shear strength of joints and aging time[61]

效 72 h 后，Sn-10%Ni 焊点只存在 Ni_3Sn_4，其强度达 68.72 MPa；Sn-24%Ni 和 Sn-30%Ni 的焊点时效后，Ni_3Sn_4 晶粒粗化导致抗剪切强度略有下降[106]。SiC/Sn(20 μm)/Ni 互连结构在 250 ℃和 0.2 MPa 压力下，超声处理 8 s 后制备了等轴 Ni_3Sn_4 接头，其平均抗剪强度为 26.7 MPa，而传统 TLP 接头的强度仅为 22.8 MPa；传统 TLP 焊点断裂主要发生在柱状 Ni_3Sn_4，超声诱导 TLP 焊点的晶间断裂发生在等轴 Ni_3Sn_4 层且晶粒相互拉拔(见图 19)[107]。适当的 Ni 可以细化晶粒从而提高焊点性能，但是当 Ni 过多或者太少会导致焊点性能严重下降。因此，调控 Sn-Ni 焊点中晶粒形貌及大小等需进一步深入研究。

3 展望

采用全 IMC 焊点以代替高铅焊点，具有非常深远的学术意义和生产启示。表 1 所列为典型全 IMC 焊点的制备方法及性能，其制备方法主要为低温烧结法、固液互扩散键合、瞬态液相连接法、感应加热、电流辅助键合，焊料体系主要有 Cu-Sn、Cu-In、Sn-Ag、Sn-Ni、Sn-Bi 焊料，全 IMC 主要集中在 Cu_3Sn、Cu_6Sn_5、$Cu_{10}Sn_3$、$Cu_{43}Sn_7$、$Cu_{19}Sn$、$Cu_{11}In_9$、Cu_7In_3、Ag_3Sn、$(Cu，Ni)_6Sn_5$、Ni_3Sn_4 等单种或多种 IMC。对于传统的低温烧结法、TLP、SLID 等工艺，由于键合时间太长，在实际生产过程中无法满足生产效能的需要，同时在键合过程中

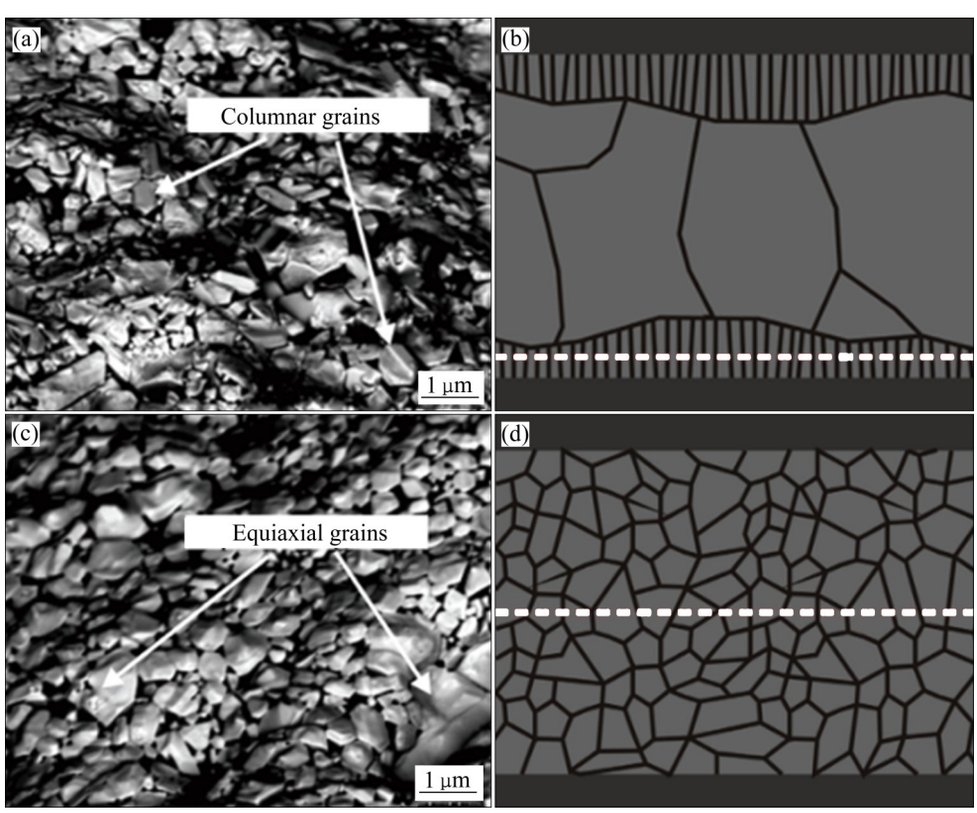

图19 Ni_3Sn_4 焊点的 SEM 顶视图和断口示意图[107]

Fig. 19 Top-view SEM images((a), (c)) and schematics((b), (d)) of fracture surfaces for Ni_3Sn_4 joints formed by different bonding progresses[107]: (a), (b) Traditional TLP bonding process; (c), (d) Ultrasound-induced TLP bonding process

会因相变而产生孔洞等缺陷，造成可靠性下降；而超声辅助TLP、电迁移、感应加热、高频磁场等方法可以快速制备IMC焊点，但制备方法苛刻、全IMC组成不可控，接头同样存在孔洞等缺陷。不同体系连接层的材料主要集中在Cu-Sn体系，Cu-In体系相对于Cu-Sn而言具有更低的键合温度，更加优异的成键性能，但In属于稀有金属，故主要应用于特殊环境制备耐高温接头。目前Cu-Sn、Cu-In、Sn-Ag、Sn-Ni等体系其全IMC接头仍然存在空洞，接头强度不高，高温服役的可靠性相对较差等问题。基于上述问题，本文作者认为：

1) 在焊料体系方面，研究者长期关注以锡基焊料为主的全IMC焊料体系，如Cu-Sn、Cu-In、Sn-Ag、Sn-Ni、Sn-Bi焊料等，对接头结构缺乏整体思考，本文作者认为研究应结合Cu-Cu接头的结构特点和基体材料的性能，开发更多基于锡基、铜基、锡铜基二元或三元焊料体系；从全IMC形成过程来看，研究应更多的关注焊料的状态、尺寸、制备方法及更多关注扩散速度快的元素，通过改变焊料状态和尺寸进一步缩短IMC形成过程中原子迁移距离，通过优化焊料尺寸和制备方法来降低IMC形成过程或服役中因原子迁移而留下的空洞，通过激活或诱导焊料中重点原子进而引发新的原子反应。

2) 在制备方法方面，研究者习惯把接头作为一个整体，进行低温烧结、固液互扩散键合、瞬态液相连接等制备全IMC，而基于器件耐热要求，制备温度不能太高。当采用低的制备温度，原子扩散受到影响，IMC制备时间长，同时高温服役时又发生不同的扩散行为，缺陷增多。本文作者认为在制备全IMC接头时，可把焊料和母材看为两个相互联系

表1　典型的全IMC焊点制备方法及性能

Table 1　Typical full-IMC solder joint preparation methods and performance

Researchers	Methods and parameters	IMC	Defect	Shear strength/MPa
LEE et al.[44]	SLID (300 ℃+2 MPa+2 h)	Cu_3Sn	No	55
ZHAO et al.[94]	Ultrasonic-assisted TLP (350 W+20 kHz+250 ℃+0.5 MPa+8 s)	Cu_3Sn	Void	65
LIU et al.[83]	Ultrasonic-assisted TLP (600 W+20 kHz+250 ℃+0.4 MPa+30 s)	Cu_6Sn_5 and Cu_3Sn	Cavitaation	60
BRINCKER et al.[92]	TLP (255 ℃+25 MPa+60 min)	Cu_6Sn_5 and Cu_3Sn	Less void	90−95
GUO et al.[39]	Sinter (300 ℃+20 min)	$Cu_{10}Sn_3$	Less void and Crack	26.8
LIU et al.[78]	Assisted by electric current bonding (1.5×10^4 A/cm^2+200 ms+0.08 MPa)	Cu_3Sn and $Cu_{41}Sn_{11}$	No	63.4
LIU et al.[70]	Induction heating (300 kHz+0.7 MPa+2 min)	$Cu_{43}Sn_7$ and $Cu_{19}Sn$	Less void	80−90
YANG et al.[96]	TLP (260 ℃+5 MPa+30 min)	$Cu_{11}In_9$	Void	16.35
LEE et al.[85]	TLP (200 ℃+50 MPa+300 s) and aging (300 ℃+500 h)	Cu_7In_3	No	23−25
SHAO et al.[88]	Ultrasonic-assisted TLP (300 W+20 kHz+0.5 MPa+310 ℃+15 s)	Ag_3Sn	No	53.7
BAO et al.[98]	TLP (300 ℃+60 min)	Ag_3Sn and Cu_3Sn	Void	72.3
Hwang et al.[60]	TLP (300 ℃+2 h)	Ag_3Sn and Cu_6Sn_5 and Cu_3Sn	Less void	48.9
DONG et al.[104]	TLP (260 ℃+80 g+120 min)	$(Cu, Ni)_6Sn_5$ and Cu_3Sn	No	49.8
TIAN et al.[90]	TG-TLP (200−330 ℃, 17 min)	Ni_3Sn_4	No	180.8
JI et al.[106]	Ultrasonic-assisted TLP (35 kHz+500 W+0.4 MPa+250 ℃+10 s)	Ni_3Sn_4	No	43.4

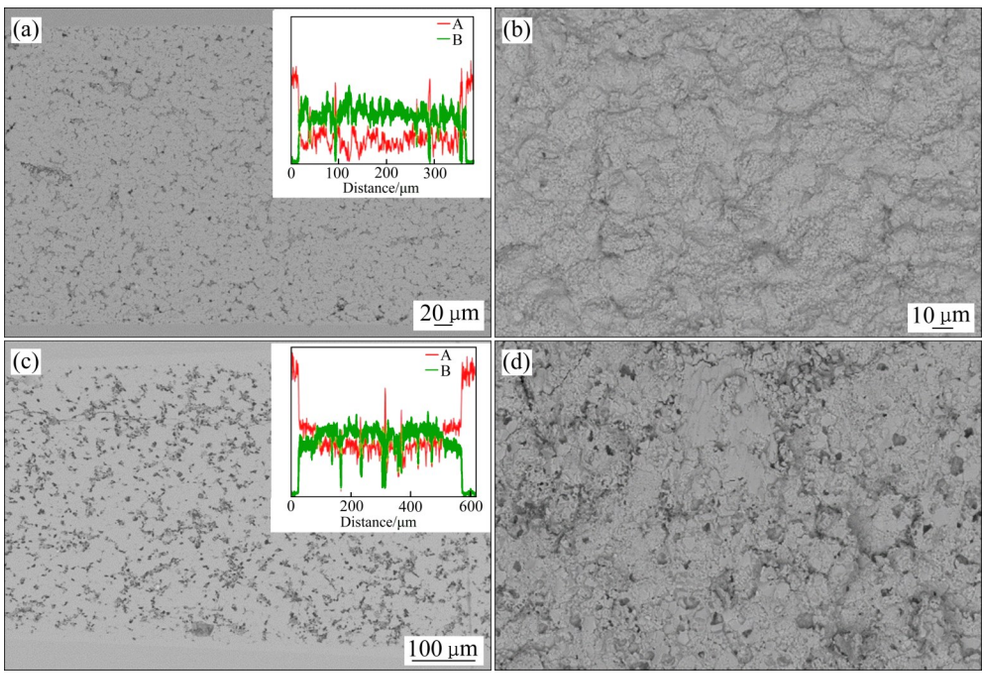

图20 在260 ℃下保温5 min获得的IMC焊点及其断口和在400 ℃时效24 h的IMC焊点及其断口形貌

Fig. 20 IMC joints (a) and its fracture morphology (b) held at 260 ℃ for 5 min and IMC joints (c) and its fracture morphology (d) aged at 400 ℃ for 24 h

的微个体，对焊料进行瞬态高功率加热，如飞秒激光、激光局部加热、感应加热等，同时对母材进行高功率制冷，把接头构造为一个冷热微循环。此外，制备过程中适当辅助振动和压力，可增加碰撞和扩散几率，缩短扩散距离。

基于在上述思想，重庆理工大学近期选用混合焊料于260 ℃下保温5 min成功地制备了Cu/Cu单一的IMC焊点(见图20)，垂直于焊缝方向显微硬度为328.45 HV，平行于焊缝方向显微硬度为326.97 HV，焊点剪切强度为36.38 MPa；在400 ℃时效24 h时，焊点剪切强度提高到41.86 MPa，时效前后断口均呈韧脆混合断裂，完全满足全IMC焊点制备和性能需求, 为其产业化应用打下了坚实的基础。

今后，应开发更多的低温快速制备全IMC的焊料体系，建立具有普适性的全IMC焊料体系设计策略；同时加强全IMC焊点制备工艺方面的研究，获得相对系统、稳定的全IMC焊点制备工艺；再次，应加强全IMC焊点可靠性，特别是高温、快速温变等极端条件下焊点可靠性方面的研究；此外，加强免热沉陶瓷与免热沉陶瓷、金属间如Si/Cu、SiC/Cu、Si/Si、SiO_2/Cu等全IMC焊料体系的开发。

REFERENCES

[1] ZHAO Y, WU Y, EVANS K, et al. Evaluation of Ag sintering die attach for high temperature power module applications[C]// 2014 15th International Conference on Electronic Packaging Technology. Chengdu: IEEE, 2014: 200−204.

[2] CHIN H S, CHEONG K Y, ISMAIL A B. A review on die attach materials for SiC-based high-temperature power devices[J]. Metallurgical and Materials Transactions B, 2010, 41(4): 824−832.

[3] WERNER M R, FAHRNER W R. Review on materials, microsensors, systems and devices for high-temperature and harsh-environment applications[J]. IEEE Transactions on Industrial Electronics, 2001, 48(2): 249−257.

[4] ZHANG H, MINTER J, LEE N C. A brief review on high-temperature, Pb-free die-attach materials[J]. Journal of Electronic Materials, 2019, 48(1): 201−210.

[5] YAMADA Y, TAKAKU Y, YAGI Y, et al. Pb-free high temperature solder joints for power semiconductor devices[J]. Transactions of the Japan Institute of Electronics Packaging, 2009, 2(1): 79−84.

[6] KIM S J, KIM K S, KIM S S, et al. Characteristics of Zn-Al-

Cu alloys for high temperature solder application[J]. Materials Transactions, 2008, 49(7): 1531−1536.

[7] FEI X, QIU X, LI Y. Effects of Sn element on microstructure and properties of Zn-Cu-Bi-Sn high-temperature solder[J]. Transactions of Nonferrous Metals Society of China, 2015, 25(3): 879−884.

[8] 韦习成, 鞠国魁, 孙 鹏, 等. 高温、高湿环境中时效时 Sn-Zn 基无铅焊点的显微组织演化[J]. 中国有色金属学报, 2006 , 16(7): 1177−1183.
WEI Xi-cheng, JU Guo-kui, SUN Peng. Microstructure evolution of Sn-Zn based lead-free solder joints aged in humid atmosphere at high temperature[J]. Transactions of Nonferrous Metals Society of China, 2006, 16(7): 1177−1183.

[9] SUGANUMA K, KIM S J, KIM K S. High-temperature lead-free solders: Properties and possibilities[J]. JOM Journal of the Minerals, Metals and Materials Society, 2009, 61(1): 64−71.

[10] PING W U. Effects of Zn addition on mechanical properties of eutectic Sn-58Bi solder during liquid-state aging[J]. Transactions of Nonferrous Metals Society of China, 2015, 25(4): 1225−1233.

[11] CHIDAMBARAM V, HATTEL J, HALD J. High-temperature lead-free solder alternatives[J]. Microelectronic Engineering, 2011, 88(6): 981−989.

[12] ZHONG Y, AN R, WANG C, et al. Low temperature sintering Cu_6Sn_5 nanoparticles for superplastic and super-uniform high temperature circuit interconnections[J]. Small, 2015, 11(33): 4097−4103.

[13] MEYER J, PANCHENKO I, WAMBERA L, et al. Accelerated SLID bonding for fine-pitch interconnects with porous microstructure[C]// 2017 IEEE 67th Electronic Components and Technology Conference (ECTC). Orlando: IEEE, 2017: 405−410.

[14] SHARIF A, GAN C L, CHEN Z. Transient liquid phase Ag-based solder technology for high-temperature packaging applications[J]. Journal of Alloys and Compounds, 2014, 587: 365−368.

[15] CHEN W Y, SONG R W, DUH J G. Grain structure modification of Cu-Sn IMCs by applying Cu-Zn UBM on transient liquid-phase bonding in novel 3D-IC technologies[J]. Intermetallics, 2017, 85: 170−175.

[16] LIU X, ZHOU S, NISHIKAWA H. Thermal stability of low-temperature sintered joint using Sn-coated Cu particles during isothermal aging at 250 ℃ [J]. Journal of Materials Science: Materials in Electronics, 2017, 28(17): 12606−12616.

[17] BORDÈRE S, FEUILLET E, DIOT J L, et al. Understanding of void formation in Cu/Sn-Sn/Cu system during transient liquid phase bonding process through diffusion modeling[J]. Metallurgical and Materials Transactions B, 2018, 49(6): 3343−3356.

[18] DENG Y, ZHONG W, XU H. Interlayer design for partial transient liquid phase bonding of titanium and copper[J]. Materials Science and Engineering A, 2021, 807: 140879.

[19] BAJWA A A, WILDE J. Reliability modeling of Sn-Ag transient liquid phase die-bonds for high-power SiC devices[J]. Microelectronics Reliability, 2016, 60: 116−125.

[20] LI J F, AGYAKWA P A, JOHNSON C M. Suitable thicknesses of base metal and interlayer, and evolution of phases for Ag/Sn/Ag transient liquid-phase joints used for power die attachment[J]. Journal of Electronic Materials, 2014, 43(4): 983−995.

[21] LIS A, LEINENBACH C. Effect of process and service conditions on TLP-bonded components with (Ag, Ni-) Sn interlayer combinations[J]. Journal of Electronic Materials, 2015, 44(11): 4576−4588.

[22] LI J F, AGYAKWA P A, JOHNSON C M. Interfacial reaction in Cu/Sn/Cu system during the transient liquid phase soldering process[J]. Acta Materialia, 2011, 59(3): 1198−1211.

[23] SOMMADOSSI S, GUST W, MITTEMEIJER E J. Phase characterisation and kinetic behaviour of diffusion soldered Cu/In/Cu interconnections[J]. Materials Science and Technology, 2003, 19(4): 528−534.

[24] XIONG M, ZHANG L, SUN L, et al. Effect of Cu/Zn/Al particles addition on microstructure of Cu/Sn58Bi/Cu TLP bonding solder joints[J]. Vacuum, 2019, 167: 301−306.

[25] MIN K D, JUNG K H, LEE C J, et al. Enhancement of electrochemical and thermal bonding reliability by forming a Cu_3Sn intermetallic compound using Cu and Sn-58Bi[J]. Journal of Alloys and Compounds, 2021, 857: 157595.

[26] MOKHTARI O, NISHIKAWA H. The shear strength of transient liquid phase bonded Sn-Bi solder joint with added Cu particles[J]. Advanced Powder Technology, 2016, 27(3): 1000−1005.

[27] MOKHTARI O, NISHIKAWA H. Transient liquid phase bonding of Sn-Bi solder with added Cu particles[J]. Journal of Materials Science: Materials in Electronics, 2016, 27(5): 4232−4244.

[28] WANG H, FANG J, XU Z, et al. Improvement of Ga and Zn alloyed Sn-0.7Cu solder alloys and joints[J]. Journal of Materials Science: Materials in Electronics, 2015, 26(6): 3589−3595.

[29] NISHIKAWA H, PIAO J Y, TAKEMOTO T. Interfacial reaction between Sn-0.7Cu (-Ni) solder and Cu substrate[J]. Journal of Electronic Materials, 2006, 35(5): 1127−1132.

[30] TIAN Y, HANG C, ZHAO X, et al. Phase transformation and fracture behavior of Cu/In/Cu joints formed by solid–liquid interdiffusion bonding[J]. Journal of Materials Science: Materials in Electronics, 2014, 25(9): 4170−4178.

[31] ZHAO X, TIAN Y, WANG N. Shearing properties of low temperature Cu-In Solid-Liquid Interdiffusion in 3D package [C]// 2013 14th International Conference on Electronic Packaging Technology. Dalian: IEEE, 2013: 143−147.

[32] JEONG S W, KIM J H, LEE H M. Effect of cooling rate on growth of the intermetallic compound and fracture mode of near-eutectic Sn-Ag-Cu/Cu pad: Before and after aging[J]. Journal of Electronic Materials, 2004, 33(12): 1530−1544.

[33] JO Y H, LEE J W, SEO S K, et al. Demonstration and characterization of Sn-3.0Ag-0.5Cu/Sn-57Bi-1Ag combination solder for 3D multistack packaging[J]. Journal of Electronic Materials, 2008, 37(1): 110−117.

[34] ZHANG W, CAO Y, HUANG J, et al. Ultrasonic-accelerated metallurgical reaction of Sn/Ni composite solder: Principle, kinetics, microstructure, and joint properties[J]. Ultrasonics Sonochemistry, 2020, 66: 105090.

[35] TIAN R, HANG C, TIAN Y, et al. Brittle fracture induced by phase transformation of Ni-Cu-Sn intermetallic compounds in Sn-3Ag-0.5Cu/Ni solder joints under extreme temperature environment[J]. Journal of Alloys and Compounds, 2019, 777: 463−471.

[36] WANG F, CHEN H, HUANG Y, et al. Recent progress on the development of Sn-Bi based low-temperature Pb-free solders[J]. Journal of Materials Science: Materials in Electronics, 2019, 30(4): 3222−3243.

[37] CHEN X, XUE F, ZHOU J, et al. Effect of In on microstructure, thermodynamic characteristic and mechanical properties of Sn-Bi based lead-free solder[J]. Journal of Alloys and Compounds, 2015, 633: 377−383.

[38] LI K, WANG X. Effect of pulsed current on the microstructure evolution of Cu-Sn intermetallic compounds[J]. Materials Science and Technology, 2017, 33(17): 2097−2101.

[39] GUO L, LIU W, JI X, et al. Facile synthesis of $Cu_{10}Sn_3$ nanoparticles and their sintering behavior for power device packaging[J]. Results in Materials, 2021, 10: 100187.

[40] GUO L, LIU W, WANG C. Preparation and sintering properties of $Cu_{10}Sn_3$ IMCs nanopaste as die attach material for high temperature power electronics[J]. Materials Letters, 2021, 282: 128845.

[41] 田艳红 . 基于 3D 封装芯片互连的固液互扩散低温键合机理及可靠性研究[J]. 机械制造文摘-焊接分册, 2013(1): 18−20.
TIAN Yan-hong. Research on solid-liquid interdiffusion low-temperature bonding mechanism and reliability based on 3D package chip interconnection[J]. Welding Digest of Machinery Manufacturing, 2013(1): 18−20.

[42] YAO P, LI X, JIN F, et al. Morphology transformation on Cu_3Sn grains during the formation of full Cu_3Sn solder joints in electronic packaging[J]. Soldering & Surface Mount Technology, 2018, 30(1): 14−25.

[43] YAO P, LI X, HAN X, et al. Shear strength and fracture mechanism for full Cu-Sn IMCs solder joints with different Cu_3Sn proportion and joints with conventional interfacial structure in electronic packaging[J]. Soldering & Surface Mount Technology, 2019, 31(1): 6−19.

[44] LEE B S, YOON J W. Cu-Sn intermetallic compound joints for high-temperature power electronics applications[J]. Journal of Electronic Materials, 2018, 47(1): 430−435.

[45] HANG C, TIAN Y, ZHANG R, et al. Phase transformation and grain orientation of Cu-Sn intermetallic compounds during low temperature bonding process[J]. Journal of Materials Science: Materials in Electronics, 2013, 24(10): 3905−3913.

[46] LEMETTRE S, SEOK S, ISAC N, et al. Low temperature solid-liquid interdiffusion wafer and die bonding based on PVD thin Sn/Cu films[J]. Microsystem Technologies, 2017, 23(9): 3893−3899.

[47] LIN J C, HUANG L W, JANG G Y, et al. Solid-liquid interdiffusion bonding between In-coated silver thick films[J]. Thin Solid Films, 2002, 410(1/2): 212−221.

[48] FUKUMOTO S, MIYAKE K, TATARA S, et al. Solid-liquid interdiffusion bonding of copper using Ag-Sn layered films [J]. Materials Transactions, 2015, 56(7): 1019−1024.

[49] LI Z L, TIAN H, DONG H J, et al. The nucleation-controlled intermetallic grain refinement of Cu-Sn solid-liquid interdiffusion wafer bonding joints induced by addition of Ni particles[J]. Scripta Materialia, 2018, 156: 1−5.

[50] LARSSON A, TOLLEFSEN T A, AASMUNDTVEIT K E.

Ni-Sn solid liquid interdiffusion (SLID) bonding—process, bond characteristics and strength[C]// 2016 6th Electronic System-Integration Technology Conference (ESTC). Grenoble: IEEE, 2016: 1−6.

[51] SUN L, CHEN M, ZHANG L. Microstructure evolution and grain orientation of IMC in Cu-Sn TLP bonding solder joints[J]. Journal of Alloys and Compounds, 2019, 786: 677−687.

[52] 邵华凯, 吴爱萍, 邹贵生. Cu-Sn体系LTTLP连接焊点强度与断口分析[J]. 焊接学报, 2017, 38(3): 13−16.
SHAO Hua-kai, WU Ai-ping, ZOU Gui-sheng. Analysis of solder joint strength and fracture of Cu-Sn system LTTLP[J]. Transactions of the China Welding Institution, 2017, 38(3): 13−16.

[53] WU Z, CAI J, WANG Q, et al. Wafer-level hermetic package by low-temperature Cu/Sn TLP bonding with optimized Sn thickness[J]. Journal of Electronic Materials, 2017, 46(10): 6111−6118.

[54] MO L, WU F, LIU C. Growth kinetics of IMCs in Cu-Sn intermetallic joints during isothermal soldering process[C]// 2015 IEEE 65th Electronic Components and Technology Conference (ECTC). San Diego: IEEE, 2015: 1854−1858.

[55] SUN F, PAN Z, LIU Y, et al. Microstructure evolution and shear strength of full Cu3Sn-microporous copper composite joint by thermo-compression bonding[J]. Soldering & Surface Mount Technology, 2021, 33(5): 274−280.

[56] 董红杰, 赵洪运, 宋晓国, 等. Ni-Cu低温TLP扩散连接接头组织及性能[J]. 焊接学报, 2017, 38(10): 125−128.
DONG Hong-jie, ZHAO Hong-yun, SONG Xiao-guo, et al. Microstructure and properties of Ni-Cu low temperature TLP diffusion bonding joint[J]. Transactions of The China Welding Institution, 2017, 38(10): 125−128.

[57] LEE B S, KO Y H, LEE C W, et al. Comparative study of nickel-tin and copper-tin transient liquid phase bondings for power electronics packaging[C]// 2016 6th Electronic System-Integration Technology Conference (ESTC). Grenoble: IEEE, 2016: 1−3.

[58] CHU K, SOHN Y, MOON C. A comparative study of Cn/Sn/Cu and Ni/Sn/Ni solder joints for low temperature stable transient liquid phase bonding[J]. Scripta Materialia, 2015, 109: 113−117.

[59] MIN K D, JUNG K H, LEE C J, et al. Pressureless transient liquid phase sintering bonding in air using Ni and Sn-58Bi for high-temperature packaging applications[J]. Journal of Materials Science: Materials in Electronics, 2019, 30(20): 18848−18857.

[60] HWANG B U, MIN K D, LEE C J, et al. Pressureless transient liquid phase bonding using SAC305 with hybrid Ag particles and its reliability under high-temperature storage test[J]. Materialia, 2020, 12: 100808.

[61] SHAO H, WU A, BAO Y, et al. Microstructure evolution and mechanical properties of Cu/Sn/Ag TLP-bonded joint during thermal aging[J]. Materials Characterization, 2018, 144: 469−478.

[62] FENG H, HUANG J, PENG X, et al. Microstructural evolution of Ni-Sn transient liquid phase sintering bond during high-temperature aging[J]. Journal of Electronic Materials, 2018, 47(8): 4642−4652.

[63] MIN K D, LEE C J, HWANG B U, et al. Hybrid transient liquid phase sintering bonding of Sn-3.0 Ag-0.5 Cu solder with added Cu and Ni for Cu-Ni bonding[J]. Applied Surface Science, 2021, 551: 149396.

[64] JUNG K H, MIN K D, LEE C J, et al. Pressureless die attach by transient liquid phase sintering of Cu nanoparticles and Sn-58Bi particles assisted by polyvinylpyrrolidone dispersant [J]. Journal of Alloys and Compounds, 2019, 781: 657−663.

[65] TATSUMI H, LIS A, YAMAGUCHI H, et al. Evolution of transient liquid-phase sintered Cu-Sn skeleton microstructure during thermal aging[J]. Applied Sciences, 2019, 9(1): 157.

[66] LIU X, HE S, NISHIKAWA H. Thermally stable Cu_3Sn/Cu composite joint for high-temperature power device[J]. Scripta Materialia, 2016, 110: 101−104.

[67] LI J F, AGYAKWA P A, JOHNSON C M. Kinetics of Ag_3Sn growth in Ag-Sn-Ag system during transient liquid phase soldering process[J]. Acta Materialia, 2010, 58(9): 3429−3443.

[68] BOSCO N S, ZOK F W. Critical interlayer thickness for transient liquid phase bonding in the Cu-Sn system[J]. Acta Materialia, 2004, 52(10): 2965−2972.

[69] YIN Z, SUN F, GUO M. The fast formation of Cu-Sn intermetallic compound in Cu/Sn/Cu system by induction heating process[J]. Materials Letters, 2018, 215: 207−210.

[70] LIU W, WANG Y, WANG C, et al. Copper-tin reaction and preparation of microsolder joints under high frequency alternating magnetic field[C]// 2017 18th International Conference on Electronic Packaging Technology (ICEPT). Harbin: IEEE, 2017: 1592−1594.

[71] HAN X, LI X, YAO P, et al. Influence of ultrasounds on interfacial microstructures of Cu-Sn solder joints[J]. Soldering & Surface Mount Technology, 2021, 33(4):

206−214.

[72] JI H, QIAO Y, LI M. Rapid formation of intermetallic joints through ultrasonic-assisted die bonding with Sn-0.7Cu solder for high temperature packaging application[J]. Scripta Materialia, 2016, 110: 19−23.

[73] LI Z, LI M, XIAO Y, et al. Ultrarapid formation of homogeneous Cu_6Sn_5 and Cu_3Sn intermetallic compound joints at room temperature using ultrasonic waves[J]. Ultrasonics Sonochemistry, 2014, 21(3): 924−929.

[74] HAN X, LI X, YAO P, et al. Interfacial microstructure evolution for Cu/Cu_3Sn/Cu Solder Joints during ultrasonic-assisted TLP soldering process[C]// 2019 IEEE 21st Electronics Packaging Technology Conference (EPTC). Singapore: IEEE, 2019: 355−359.

[75] LIU J H, ZHAO H Y, LI Z L, et al. Study on the microstructure and mechanical properties of Cu-Sn intermetallic joints rapidly formed by ultrasonic-assisted transient liquid phase soldering[J]. Journal of Alloys and Compounds, 2017, 692: 552−557.

[76] MUNIR Z A, ANSELMI-TAMBURINI U, OHYANAGI M. The effect of electric field and pressure on the synthesis and consolidation of materials: A review of the spark plasma sintering method[J]. Journal of Materials Science, 2006, 41(3): 763−777.

[77] MUNIR Z A, QUACH D V, OHYANAGI M. Electric current activation of sintering: A review of the pulsed electric current sintering process[J]. Journal of the American Ceramic Society, 2011, 94(1): 1−19.

[78] LIU B, TIAN Y, WANG C, et al. Ultrafast formation of unidirectional and reliable Cu_3Sn-based intermetallic joints assisted by electric current[J]. Intermetallics, 2017, 80: 26−32.

[79] GUO M, SUN F, YIN Z. Microstructure evolution and growth behavior of Cu/SAC105/Cu joints soldered by thermo-compression bonding[J]. Soldering & Surface Mount Technology, 2019, 30(4): 227−232.

[80] JEONG S E, JUNG S B, YOON J W. A study of the growth rate of Cu-Sn intermetallic compounds for transient liquid phase bonding during isothermal aging[C]// 2018 IEEE 20th Electronics Packaging Technology Conference (EPTC). Singapore: IEEE, 2018: 225−228.

[81] LI M, LI Z, XIAO Y, et al. Rapid formation of Cu/Cu_3Sn/Cu joints using ultrasonic bonding process at ambient temperature[J]. Applied Physics Letters, 2013, 102: 094104.

[82] ZHAO H Y, LIU J H, LI Z L, et al. Non-interfacial growth of Cu_3Sn in Cu/Sn/Cu joints during ultrasonic-assisted transient liquid phase soldering process[J]. Materials Letters, 2017, 186: 283−288.

[83] LIU J, ZHAO H, LI Z L, et al. The study of the growth behavior of Cu_6Sn_5 intermetallic compound in Cu/Sn/Cu interconnection system during the ultrasonic-assisted transient liquid phase soldering[C]// 2017 18th International Conference on Electronic Packaging Technology (ICEPT). Harbin: IEEE, 2017: 10−13.

[84] TIAN Y, HANG C, ZHAO X, et al. Phase transformation and fracture behavior of Cu/In/Cu joints formed by solid–liquid interdiffusion bonding[J]. Journal of Materials Science: Materials in Electronics, 2014, 25(9): 4170−4178.

[85] LEE J B, HWANG H Y, RHEE M W. Reliability investigation of Cu/In TLP bonding[J]. Journal of Electronic Materials, 2015, 44(1): 435−441.

[86] VUORINEN V, DONG H, ROSS G, et al. Wafer level solid liquid interdiffusion bonding: formation and evolution of microstructures[J]. Journal of Electronic Materials, 2021, 50(3): 818−824.

[87] LITYNSKA L, WOJEWODA J, ZIEBA P, et al. Characterization of interfacial reactions in Cu/In/Cu joints[J]. Microchimica Acta, 2004, 145(1): 107−110.

[88] SHAO H, WU A, BAO Y, et al. Rapid Ag/Sn/Ag transient liquid phase bonding for high-temperature power devices packaging by the assistance of ultrasound[J]. Ultrasonics Sonochemistry, 2017, 37: 561−570.

[89] FENG H, HUANG J, PENG X, et al. A study of Ni_3Sn_4 growth dynamics in Ni-Sn TLPS bonding process by differential scanning calorimetry[J]. Thermochimica Acta, 2018, 663: 53−57.

[90] TIAN Y, FANG H, REN N, et al. Reliable single-phase micro-joints with high melting point for 3D TSV chip stacking[J]. Journal of Alloys and Compounds, 2020, 828: 154468.

[91] YOON S W, GLOVER M D, SHIOZAKI K. Nickel-tin transient liquid phase bonding toward high-temperature operational power electronics in electrified vehicles[J]. IEEE Transactions on Power Electronics, 2012, 28(5): 2448−2456.

[92] BRINCKER M, SÖHL S, EISELE R, et al. Strength and reliability of low temperature transient liquid phase bonded Cu/Sn/Cu interconnects[J]. Microelectronics Reliability, 2017, 76: 378−382.

[93] BOSCO N S, ZOK F W. Strength of joints produced by transient liquid phase bonding in the Cu-Sn system[J]. Acta

Materialia, 2005, 53(7): 2019−2027.

[94] ZHAO H Y, LIU J H, LI Z L, et al. A comparative study on the microstructure and mechanical properties of Cu_6Sn_5 and Cu_3Sn joints formed by TLP soldering with/without the assistance of ultrasonic waves[J]. Metallurgical and Materials Transactions A, 2018, 49(7): 2739−2749.

[95] PAN H, HUANG J, JI H, et al. Enhancing the solid/liquid interfacial metallurgical reaction of Sn+Cu composite solder by ultrasonic-assisted chip attachment[J]. Journal of Alloys and Compounds, 2019, 784: 603−610.

[96] YANG L, WANG G, XIONG Y, et al. Investigation of Cu particles size and bonding time on the microstructure and shear property of Cu/In-45Cu/Cu solder joints[J]. Materials Research Express, 2020, 7: 016314.

[97] YANG L, QIAO J, ZHANG Y C, et al. Effect of bonding time on microstructure and shear property of Cu/In-50Ag/Cu TLP solder joints[J]. Journal of Electronic Materials, 2020, 49(7): 4300−4306.

[98] BAO Y, WU A, SHAO H, et al. Effect of powders on microstructures and mechanical properties for Sn-Ag transient liquid phase bonding in air[J]. Journal of Materials Science: Materials in Electronics, 2018, 29(12): 10246−10257.

[99] SHAO H, WU A, BAO Y, et al. Interfacial reaction and mechanical properties for Cu/Sn/Ag system low temperature transient liquid phase bonding[J]. Journal of Materials Science: Materials in Electronics, 2016, 27(5): 4839−4848.

[100] SHAO H, WU A, BAO Y, et al. Elimination of pores in Ag-Sn TLP bonds by the introduction of dissimilar intermetallic phases[J]. Journal of Materials Science, 2017, 52(6): 3508−3519.

[101] SHAO H, WU A, BAO Y, et al. Microstructure characterization and mechanical behavior for Ag_3Sn joint produced by foil-based TLP bonding in air atmosphere[J]. Materials Science and Engineering A, 2017, 680: 221−231.

[102] GUO Q, SUN S, ZHANG Z, et al. Microstructure evolution and mechanical strength evaluation in Ag/Sn/Cu TLP bonding interconnection during aging test[J]. Microelectronics Reliability, 2018, 80: 144−148.

[103] LEE B S, HYUN S K, YOON J W. Cu-Sn and Ni-Sn transient liquid phase bonding for die-attach technology applications in high-temperature power electronics packaging[J]. Journal of Materials Science: Materials in Electronics, 2017, 28(11): 7827-7833.

[104] DONG H J, LI Z L, SONG X G, et al. Grain morphology and mechanical strength of high-melting-temperature intermetallic joints formed in asymmetrical Ni/Sn/Cu system using transient liquid phase soldering process[J]. Journal of Alloys and Compounds, 2017, 723: 1026−1031.

[105] DONG H J, LI Z L, SONG X G, et al. Grain morphology evolution and mechanical strength change of intermetallic joints formed in Ni/Sn/Cu system with variety of transient liquid phase soldering temperatures[J]. Materials Science and Engineering A, 2017, 705: 360−365.

[106] JI H, LI M, MA S, et al. Ni_3Sn_4-composed die bonded interface rapidly formed by ultrasonic-assisted soldering of Sn/Ni solder paste for high-temperature power device packaging[J]. Materials and Design, 2016, 108: 590−596.

[107] LI Z L, DONG H J, SONG X G, et al. Rapid formation of Ni_3Sn_4 joints for die attachment of SiC-based high temperature power devices using ultrasound-induced transient liquid phase bonding process[J]. Ultrasonics Sonochemistry, 2017, 36: 420−426.

Progress advances in full IMC solder joints for power electronic

LIU Cong[1], GAN Gui-sheng[1, 2], JIANG Zhao-qi[1], HUANG Tian[1], MA Peng[1], CHEN Shi-qi[1], XU Qian-zhu[1], BAO Cheng-li[1], CHENG Da-yong[2], WU Yi-ping[3]

(1. Chongqing Municipal Engineering Research Center of Institutions of Higher Education for Special Welding Materials and Technology, Chongqing University of Technology, Chongqing 400054, China;
2. Golden Dragon Precise Copper Tube Group Inc, Chongqing 404000, China;
3. School of Materials Science and Engineering, Huazhong University of Science and Technology, Wuhan 430074, China)

Abstract: Full intermetallic compound solder joints have become the most alternative to high lead solder, Au based solder and other connecting materials utilized in high temperature environment since they can be prepared at low temperature and serve at high temperature. The characteristics of full IMC prepared by low temperature sintering, solid-liquid interdiffusion bonding and transient liquid phase method were summarized. Furthermore, the research progress of full IMC soldered by Cu/Sn, Cu/In, Sn/Ag and Sn/Ni systems was reviewed. It is reported that the main problems restricting the production and application of IMC are too long bonding time and defects such as voids caused by phase transformation. Notably, the structural characteristics and material properties of Cu-Cu joints should be considered comprehensively. In terms of solder system, more binary solder systems based on Sn, Cu and Sn-Cu or ternary solder systems were essential to be developed. Afterwards, the state, size as well as preparation methods of solders should be attached great importance. Besides, in terms of preparation method, the base metal and solder were constructed as a cold and hot microcirculation. On the one hand, the solder was subjected to transient and local high-power heating such as femtosecond laser, local laser or induction heating. On the other hand, the base metal was subjected to high-power refrigeration. Afterwards, appropriate auxiliary vibration and pressure can boost the collision diffusion probability and shorten the diffusion distance, so as to quickly obtain a single full IMC solder joint with high reliability.

Key words: full intermetallic compound; high temperature solder; preparation method; solder systems; cold and hot microcirculation

---

Foundation item: Projects(61974013, 61774066) supported by National Natural Science Foundation of China; Project(cstc2020jcyj-msxmX0819) supported by Chongqing Natural Science Foundation, China; Project(KJZD-K202101101) supported by Chongqing Municipal Education Commission Science and Technology Project Key Project, China; Project(CXQT20023) supported by Chongqing University Innovation Research Group, China; Projects(clgycx20201001, clgycx20201002) supported by Chongqing University of Technology Graduate Student Innovation Project, China

Received date: 2021-08-03; **Accepted date:** 2021-11-09

Corresponding author: GAN Gui-sheng; Tel: +86-23-62563178; E-mail: ggs@cqut.edu.cn

(编辑　王　超)